ROAD EXTRACTION FROM HIGH-RESOLUTION SATELLITE IMAGES

A THESIS SUBMITTED TO
THE GRADUATE SCHOOL OF INFORMATICS
OF
THE MIDDLE EAST TECHNICAL UNIVERSITY

BY

MERAL ÖZKAYA

IN PARTIAL FULFILLMENT OF THE REQUIREMENTS FOR THE DEGREE OF
MASTER OF SCIENCE
IN
THE DEPARTMENT OF INFORMATION SYSTEMS

JUNE 2009

Approval of the Graduate School of Informatics

_____

Prof. Dr. Nazife BAYKAL

Director

I certify that this thesis satisfies all the requirements as a thesis for the degree of Master of Science.

_____

Prof. Dr. Yasemin YARDIMCI

Head of Department

This is to certify that I have read this thesis and that in our opinion it is fully adequate, in scope and quality, as a thesis for the degree of Master of Science.

_____

Assist. Prof. Dr. Alptekin TEMİZEL

Supervisor

Examining Committee Members

Prof. Dr. Yasemin YARDIMCI	(METU, II)	_____
Assist. Prof. Dr. Alptekin TEMİZEL	(METU, II)	_____
Assoc. Prof. Dr. Şebnem DÜZGÜN	(METU, GGIT)	_____
Assist. Prof. Dr. Erhan EREN	(METU, II)	_____
Assist. Prof. Dr. Altan KOÇYİĞİT	(METU, II)	_____

I hereby declare that all information in this document has been obtained and presented in accordance with academic rules and ethical conduct. I also declare that, as required by these rules and conduct, I have fully cited and referenced all material and results that are not original to this work.

Name, Last name : Meral Özkaya

Signature : _____

ABSTRACT

ROAD EXTRACTION FROM HIGH-RESOLUTION SATELLITE IMAGES

Özkaya, Meral
MS., Department of Information Systems
Supervisor: Assist. Prof. Dr. Alptekin Temizel

June 2009, 79 pages

Roads are significant objects of an infrastructure and the extraction of roads from aerial and satellite images are important for different applications such as automated map generation and change detection. Roads are also important to detect other structures such as buildings and urban areas.

In this thesis, the road extraction approach is based on Active Contour Models for 1-meter resolution gray level images. Active Contour Models contains Snake Approach. During applications, the road structure was separated as salient-roads, non-salient roads and crossings and extraction of these is provided by using Ribbon Snake and Ziplock Snake methods. These methods are derived from traditional snake model.

Finally, various experimental results were presented. Ribbon and Ziplock Snake methods were compared for both salient and non-salient roads. Also these methods were used to extract roads in an image. While Ribbon snake is described for extraction of salient roads in an image, Ziplock snake is applied for extraction of non-salient roads. Beside these, some constant variables in literature were redefined and expressed in a formula as depending on snake approach and a new approach for extraction of crossroads were described and tried.

Keywords: Feature Extraction, Active Contour Models, Ribbon Snake, Ziplock Snake

ÖZ

YÜKSEK ÇÖZÜNÜRLÜKLÜ UYDU GÖRÜNTÜLERİNDEN YOLLARIN BULMASI

Özkaya, Meral
Yüksek Lisans., Bilişim Sistemleri Bölümü
Tez Yöneticisi: Yard. Doç Dr. Alptekin Temizel

Haziran 2009, 79 sayfa

Yollar bir altyapının önemli nesneleri olup, hava ve uydu görüntülerinden yolların bulunması, otomatik harita üretme ve zamansal değişim tespiti gibi farklı uygulamalar için önem taşımaktadır. Ayrıca yolların bulunması, örneğin binalar gibi farklı yapıların ve kentsel alanların bulunmasında önemli rol oynamaktadır.

Bu tez çalışmasında, Aktif Çevrit Modeli kullanılmıştır. Aktif Çevrit Modeli, Yılan yaklaşımını içermektedir. Kullanılan görüntüler gri seviyede olup, 1-metre çözünürlüğe sahiptir. Uygulama boyunca bir görüntüde yer alan yol üç farklı yapıya ayrılarak incelenmiştir. Bunlar belirgin yollar, belirgin olmayan yollar ve kavşaklardır. Yolların bulunmasında Şerit Yapılı Yılan ve Fermuar Yapılı Yılan

metotları kullanılmıştır. Bu metotlar geleneksel yılan yapısından türetilmiş metotlardır.

Tezin sonuç bölümünde, çeşitli deneysel sonuçlar sunuldu. Şerit ve Fermuar Yapılı Yılan metotları hem belirgin hem de belirgin olmayan yollar için test edildi. Ayrıca bu metotlar beraber kullanılarak yolların bulunması denendi. Bu metotların bir arada kullanılmasının nedenleri ve sonuçları tartışıldı. Şerit Yapılı Yılan metodu belirgin yolların bulunması için kullanılırken, Fermuar Yapılı Yılan metodu belirgin olmayan yolların bulunması için uygulanmaktadır. Bunların yanında, literatürde sabit ve kullanıcı tarafından tanımlanan bazı parametrelerin bulunması için yeni ve otomatik bir yaklaşım açıklandı. Kavşakların bulunması için yeni bir yöntem tanımlandı ve denendi.

Anahtar Kelimeler: Nesne bulma, Aktif Çevrit Modeli, Şerit Yapılı Yılan, Fermuar Yapılı Yılan

To My Family

ACKNOWLEDGEMENTS

I would like to express my gratitude to my advisor, Assist. Prof. Dr. Alptekin Temizel for patiently guidance, advice, criticism, encouragement, motivation and insight during this study. I kindly thank Prof. Dr. Yasemin Yardımcı for helpful conversations and suggestions for my thesis from the beginning.

Finally, my greatest debt is to my family to my mother Figen, my father Orhan and my younger sister Nihal for their endless love, support and encouragement.

TABLE OF CONTENTS

LIST OF TABLES

TABLE

LIST OF FIGURES

FIGURE

CHAPTER 1

INTRODUCTION

Aerial and satellite images contain valuable information about geographical structures; the planet's landforms, vegetation, natural resources or man-made objects like buildings, roads, rail-roads, bridges, etc. This information provided from images supports accurate mapping of land cover and make landscape features understandable on regional, continental, and even global scales.

In the past, information provided from aerial and satellite images were extracted manually or semi-automatically with human-computer interaction. However, automatic feature detection is preferred in recent years, in order to decrease human intervention to a minimum level. Automatic feature detection provides not only faster results but also lower cost of extraction than manual and semi-automatic type.

Roads are important objects of an infrastructure. Road data in Geographical Information Systems (GIS) has major importance for applications such as use of Global Positioning Systems (GPS) for personal car, fire and police services, military applications, traffic management, etc. Until recently, extraction of the road networks was mostly carried out manually by the operators and various methods have been proposed for semi-automatic extraction of road networks from aerial and satellite images.

Nowadays, new road detection algorithms are implemented to convert old approaches to automatic. Geometric properties of roads such as their length, width and curvature information provide information to detect roads. Many algorithms are constructed for road detection using these geometric properties.

In this thesis, the road extraction approach is based on The Active Contour Models. The Active Contour Models are defined by Kass, Witkin, & Terzopoulos (1987). Active Contour Models contain Snake Approach. Traditional snake model is separated into two representation types as analytic and discrete and uses energy minimization rule to detect roads.

Satellite images that have high resolution are publicly accessible with the advancement of Internet and imaging technologies. And also developments in technology provide to develop complex image processing algorithms. Extracting features from satellite images are becoming more popular with those developments.

Different algorithms from literature use different aerial and satellite images while extraction of a road. In this experiment, all experimented gray level images are captured from Google Maps. They have 1-meter resolution. Especially high resolution images are preferred because their geometric properties and characteristics make discovery of roads easier.

In this study, the road structure was separated as salient-roads, non-salient roads and crossings and extraction of these are done by using Ribbon Snake and Ziplock Snake. Ribbon Snake and Ziplock Snake methods are derived from traditional snake model (Laptev, Mayer, Lindeberg, Eckstein, Steger, & Baumgartner, 2000) (Neuenschwander, Fua, Szekely, & Kubler, 1997).

Salient Roads have a distinct appearance in the image. Thus salient roads are roads that are not affected or prevented by shadows and occlusion of buildings and trees in the image. Detection and verification of roads depend on roads' geometric properties such as length, width. Salient roads have steady parallel lines that have consistent length and width as homogeneity of the corresponding image region.

Figure 1: Salient road image

Non-salient roads are more difficult to detect. Typical reasons of occurrence of non salient roads in an image are shadows and occlusion of buildings and trees. To increase the detection rate on these types of roads, ziplock snake method is used. Ziplock snake needs two end points for initialization. All roads are connected into a global network. After application of ribbon snake, salient roads are extracted and these roads' start and end points can be used as ziplock snake end points during optimization step. Extraction of non-salient roads is more complicated than extraction of salient-roads. Therefore, Ziplock Snake and Ribbon Snake methods performance are compared for non-salient road detection.

After extraction of salient and non-salient roads, this information is used for crossing detection. Extractions of salient and non-salient roads provide not only minimum search space for crossing but also some points to detect crossing. Crossings link the road network together. Therefore, incomplete salient and non-salient roads are potential candidates for crossings. Crossing extraction is performed by checking incomplete adjacent roads and using the center points of the end of these incomplete roads.

Figure 2: Non-Salient road image

In this study, we use active contour models to extract salient and non-salient roads from 1-meter resolution images. Ribbon and Ziplock Snake methods are implemented for both salient and non-salient roads and their results are compared. Also Ribbon snake and Ziplock snake methods are tried together. Beside these, some constant parameters are redefined and expressed in a formula as depending on snake energy. Finally, a new approach for extraction of crossroads is described and experimentally tested.

In Chapter 2, the related works presented in the literature are summarized. And the rationales for choosing active contour models are described. Traditional snake method is explained in chapter 3. Besides this, Ribbon snake and Ziplock snake methods derived from traditional snake method and extraction of crossing method

are explained. The results of experiments using ribbon snake, Ziplock snake and extraction of crossing methods are discussed in Chapter 4. Finally, In Chapter 5, conclusions and some ideas about future work are given.

CHAPTER 2

A SUMMARY OF ROAD EXTRACTION METHODS IN THE LITERATURE

Many image processing methods are used for automatic and semi-automatic road detection applications. In this study, we classified these algorithms in six different groups. According to detection methods used figure 3 shows the classification of road extraction methods. In section 2.1, Canny, Morphology and Hough Based Methods are explained. In section 2.2, Wavelet Based methods are discussed. In section 2.3, Snake Based Methods are defined. In section 2.4, Knowledge based methods are explained. In section 2.5, Fuzzy Logic techniques are illustrated. And finally in section 2.6, the other approaches that are different from other sections, are described.

2.1 Canny, Morphology and Hough Based Applications

In Zhao, Kumagai, Nakagawa, & Shibasaki (2002), IKONOS images are used for extraction algorithms. This method has three steps that are called “Road Masks”, “Road Seeds” and “Road Line” extraction. Figure 4 shows the road extraction steps. Every method's output provides input for another one. In road mask extraction, IDL/ENVI[1] is used to extract a pixel road mask. Image pixels of a multi-spectral satellite images are classified into different groups using maximum likelihood method. In a road mask, white pixels point out the most probable road like objects.

[1] IDL and ENVI are software products for data analysis, processing and visualization. They were developed in 1980 by an alumnus. Now IDL/ENVI software products are sold by ITT Visual Information Solutions.

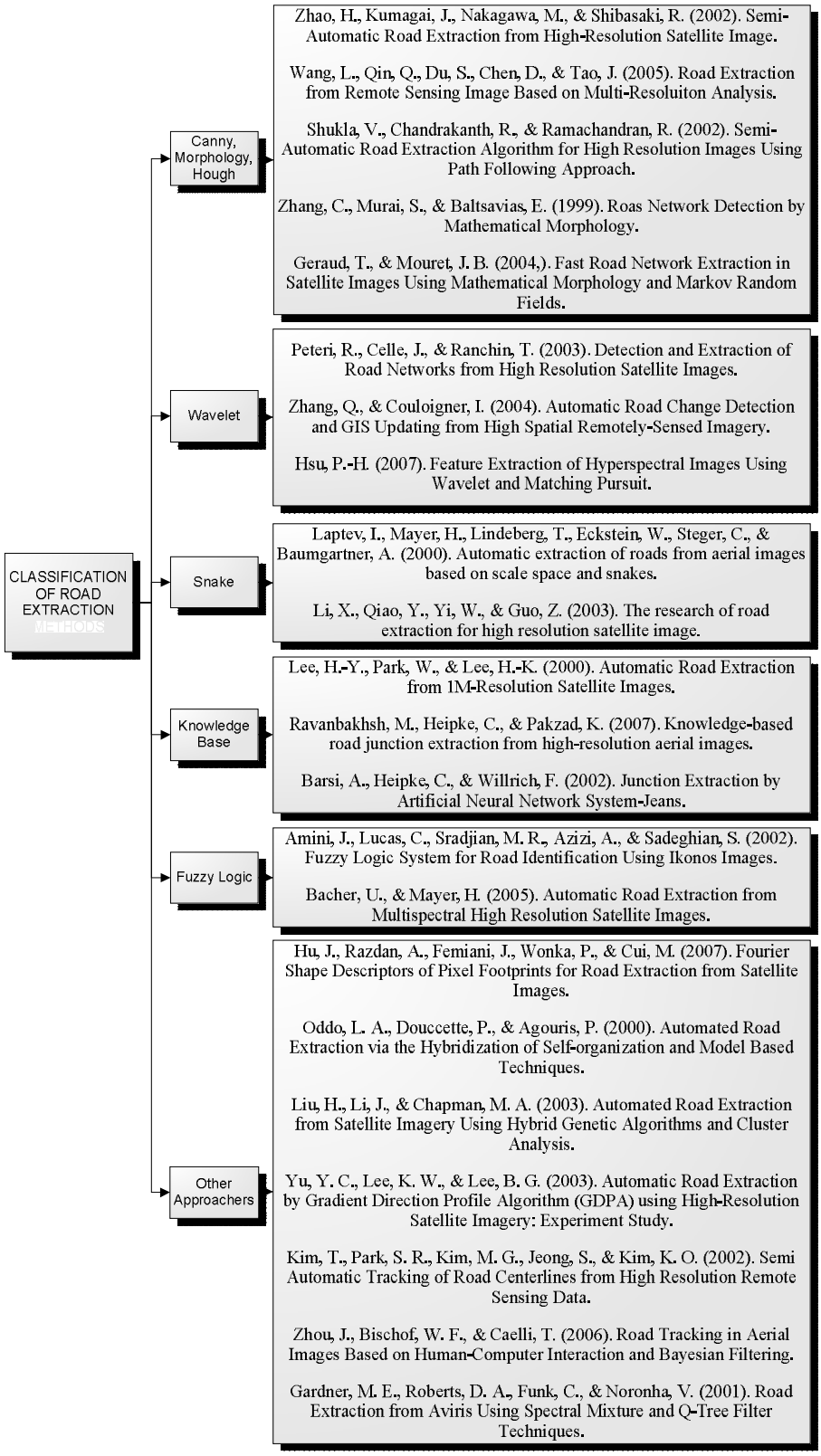

Figure 3: Classification of Road Extraction Methods

Road seeds extraction has three steps. Firstly *Canny filter* is used for edge detection. Secondly, 8-direction method is applied for all white pixels. This method depends on change of directions of pixels. Road pixels have a slow change of direction. Lastly, for joining edge line patches, in defined search space, a road edge line is joined to another, if angle between them is small than threshold.

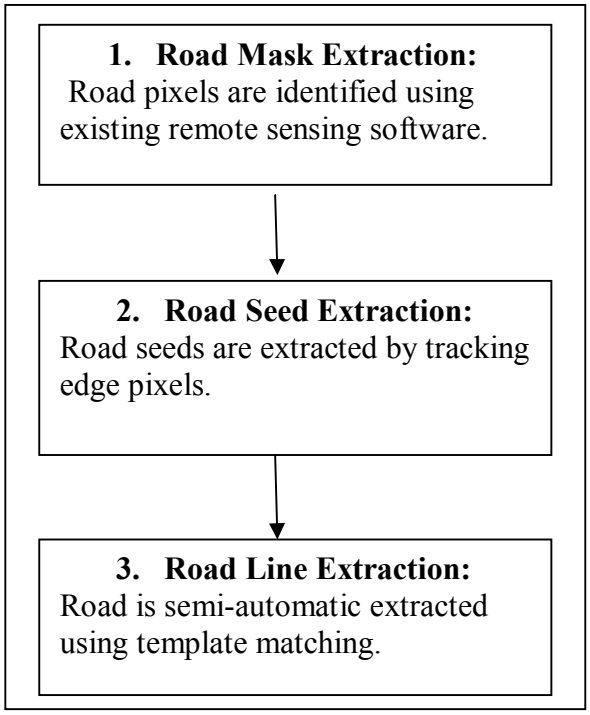

Figure 4: Road Extraction Steps

Different from the other approaches, low and mid-high resolutions of the same image are used together in Wang, Qin, Du, Chen, & Tao (2005). For each resolution, different methods are applied and their results are combined. In low resolution, canny filter is used for edge detection. After that 8-direction method is applied to detect candidate road edge pixels. Then the technique to link adjacent edges that is presented in Zhao, et al. (2002) is applied. In mid-high resolution, a simple image segmentation based on gray value threshold by way of ISODATA (Iterative Self Organizing Data Analysis Technique) classification is applied. After this segmentation, binary road image is obtained and a series of morphologic operations

are used to exclude isolated pixels on the road surface. Canny filter is used to obtain candidate road edges, and after that the image is divided into small sub-images and Hough transform is used to detect parallel road sides. Figure 5 shows these steps.

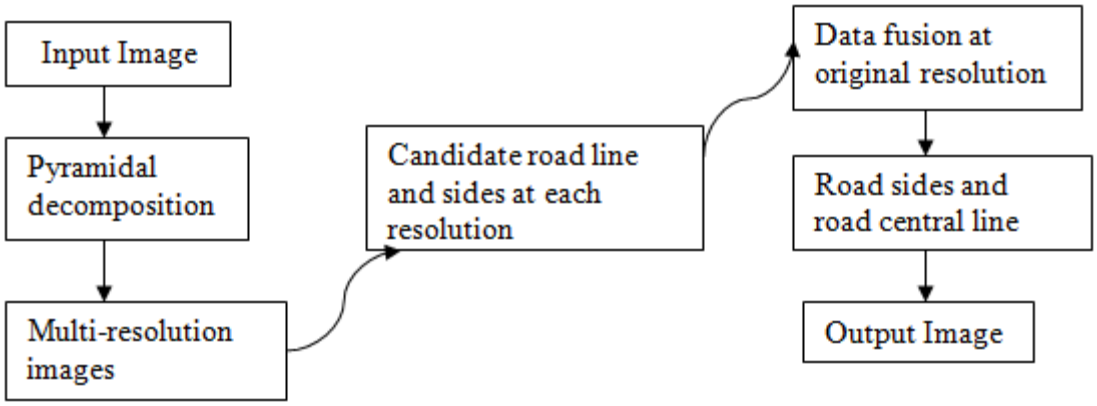

Figure 5: Extraction steps

Scale-space and edge detection applications are used as pre-processing in Shukla, Chandrakanth, & Ramachandran (2002). Scale-space is a data structure that consists of sequence of images at different scales. Canny filter is applied for edge detection. After that initial seed points are selected on the road image. At least two seed points must be defined. The width of the road is estimated as depending on initial seed points and detected edges by canny filter. Also directions of seed points are found. Cost estimation is performed for every possible three directions of each road seeds by calculating variance of the image after applying scale-space. Minimum cost path is considered the next valid path. This repeats until the end of the road.

A method for automatic road detection on 1-meter resolution images is provided using mathematical morphology in Zhang, Murai, & Baltsavias (1999). Trivial opening and granulometric techniques are applied. As pre-processing, a road is classified and segmented from background using ISODATA. As a result of ISODATA, road and other features are extracted. After that trivial opening process is executed to separate other features that have small regions because road has long

regions. Granulometric techniques support these criteria and give size distribution of object in an image. After that there might be small holes on road network and a morphological closing is applied to fill the holes.

Instead of ISODATA segmentation that is defined and applied in Zhang, et al. (1999) as a pre-processing, for road extraction, after morphological filtering, global energy minimization processes are performed in Geraud & Mouret (2004). Morphological filtering step consists of area closing followed by watershed transform. Watershed transform provides road network and using this network curve adjacency graph is obtained. A node of this graph is a shed and an edge is drawn between two nodes end of the sheds. Markov Random Field is applied for a graph labeling problem by watershed transform. That is supported by defined local energy. Finally, simulated annealing algorithm is applied to find minimum energy as depend on contextual energy.

2.2 Wavelet Based Approaches

The algorithm presented in Peteri, Celle, & Ranchin has two sequential modules (2003). First step is extraction of a topologically correct graph of the road network. Second step is reconstruction and extraction of roads as surface elements. The topologically correct graph of the road network is extracted by an algorithm that selects the best path for the potential road by a cost minimization function. After then second module is applied using this graph. This module reconstructs roads as surface elements from the graph using specific active contours with a multi-resolution analysis (MRA). Specific active contour is based on greedy algorithm and MRA is based on Wavelet transform to perform multi-resolution edge detection.

Another method using wavelet approach is explained in Zhang & Couloigner (2004). IRS-pan images are used for road extraction. Wavelet transform methodology has been developed for extraction and the feature matching and conflation techniques are

used to road change detection and updating. In this paper, the roles of wavelet transform for road extraction are mentioned. The first role obtains the multi-scale representation of original image that is provided by taking advantage of scale-space behavior of roads in combination with snakes. The second role combines wavelet transform with road extraction to detect edge pixels in the wavelet domain. After successful extraction of road feature from imagery, a feature matching is performed to identify the conjugate road nodes and road centerlines. And it does not only determine conjugate features but also it identify which parts of the road network have changed and which parts remained unchanged.

Hyper-spectral images are usually used in mining and geology, but in Hsu hyper spectral images are used for road extraction (2007). Using hyper spectral image, a feature extraction method based on matching pursuit is identified for classification. This algorithm uses greedy strategy to find an adaptive and optimal representation of data iteratively from a highly redundant dictionary that is defined as a collection of parameterized waveform. Waveforms are elementary pieces of a signal in a time frequency plain. They called as atoms. The matching pursuit algorithm use wavelet packet dictionary to detect features.

2.3 Methods Using Snakes

Aerial images are used as input for road extraction in Laptev, et al. (2000). The proposed algorithm is based on scale-space and snakes. This algorithm sequentially identifies salient roads, non-salient roads and crossings. Every step decreases the search space of the previous step. Firstly, an edge detection algorithm is applied. This might be canny filter or *detect lines* algorithm by Steger (1998). Detected lines are eliminated by comparing their lengths with a threshold. Ribbon snake provides an energy minimization method to detect salient roads. Ziplock snake method (Neuenschwander, et al. 1997) is applied for non-salient road extraction. Extraction of salient road and non-salient road reduce search space for crossing detection. Adjacent lines are detected for crossing extraction and connected each other. Figure

6 shows results of 0.5m resolution images using snake approach. According to results, correctness of figure 6(a) is %97 and completeness is %83. In figure 6(b), correctness and completeness decrease to %95 and % 72. The size of figure 6(a) is *1800x1600* pixels and the resolution is 0.46m, but the size of figure 6(b) is *4500x4500* pixels and resolution is the same with figure 6(a). As a similar result, correctness and completeness are %99 and %84 for Figure 6(c). Its size is *2000x2000* pixels and resolution is 0.37m.

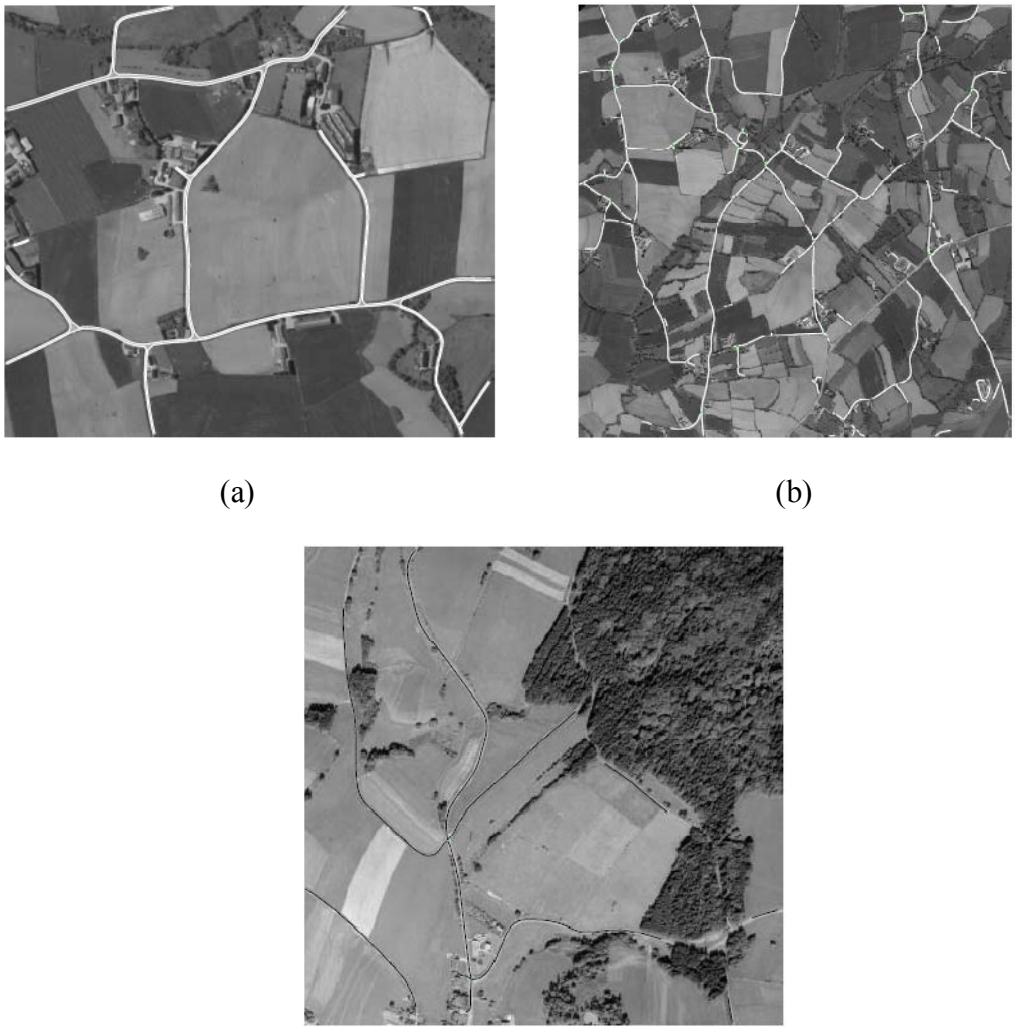

(a) (b)

(c)

Figure 6: (a) Road extraction in larger image (b) Road extraction in image "Erquy" (c) Road extraction in image "Marchetstreut" (centerlines only). Courtesy of Laptev, et al. (2000)

A multi-resolution approach using Snakes is described in Li, Qiao, Yi, & Guo (2003). SPOT-5 satellite images are used for road extraction. This algorithm consists of three steps. As pre-processing, Gaussian smoothing is applied. First step is edge detection from SPOT-5 image. Second step is road following that uses region-based tracking to eliminate road like but non-road pixels. After that the unattached segments may be obtained because of shadows, occlusions, junctions and other features that have similar features to roads. So that ribbon snake is used to connect the unattached road segments. In the last step, the extracted roads are converted to road vectors using a commercial remote sensing software, such as ENVI.

2.4 Knowledge Based Techniques

Region based strategy for the extraction of roads is applied to 1-meter resolution image in Lee, Park, & Lee (2000). Firstly, using intensity-based segmentation, image is segmented and road primitives are obtained. Secondly these road primitives are used to select road candidates using prior knowledge about the roads. These road candidates possibly include noise like shadow, building, etc and also there may be undetected road candidates. So road characteristics are obtained from these road candidates like road expansion directions and then *Profile matching* algorithm is applied.

In Ravanbakhsh, Heipke, & Pakzad, high resolution aerial images are used for road junction extraction (2007). The methodology consists of an existing geospatial data and prior knowledge is derived from it. Firstly the geospatial database is analyzed for a rough idea of road junction appearance in the image. Road junction area is separated into two parts as road arms and road junctions. Secondly the road arms are extracted using their radiometric properties, geometric properties and homogeneity. Lastly road junction reconstruction algorithm is performed. This step has inputs that are aerial image, road arms and geospatial data. In this step road junction borders are extracted and connected to adjacent road arms.

Although road junction extraction is main approach in Barsi, Heipke, & Willrich, from IKONOS satellite images, detection of road arms are necessary to extract road junction (2002). Neural network method is applied to find out a 3- or 4- arm road junction. The strategy uses both raster and vector data for extraction. Central kernel application is applied to provide raster data and to provide vector data, edge detection that uses *Deriche* algorithm is applied. Then central circle criterion is performed to evaluate the found edge vectors. In-sample and out-of-sample test is the last step of this algorithm. The final networks are evaluated.

2.5 Fuzzy Logic Structures

Like Barsi, et al. (2002) high resolution IKONOS image is used for road extraction based on a fuzzy logic system in Amini, Lucas, Sradjian, Azizi, & Sadeghian (2002). Before fuzzy-logic methods, linguistic variables and standard deviations are determined in two stages. They are histogram smoothing and detection of object. Histogram smoothing stage contains Gaussian density function as the kernel function to produce the estimated density function for data. After histogram smoothing, objects can be detectable by identification the peak and valley points using first and second derivative. This algorithm can extract %91 of the main road from high resolution satellite images.

Again for Fuzzy Logic approaches, pan-sharpened IKONOS image is used for road extraction in Bacher & Mayer (2005). Firstly training areas are obtained from linear feature using existing parallel edges. A fuzzy classification is performed to calculate a membership value for road class for each pixel. A Gaussian membership function is applied using mean and standard deviation of the gray values of the training areas. Classification provides an additional source for the extraction of road candidates. The lines are not accepted as road candidates if lines from road class contain high curvature. Final road network is decided based on a weighted graph as a given threshold. Local detour factor is calculated to detect missing connections in the

network and these missing connections is connected using Ziplock snake method. Figure 7 shows results of processes.

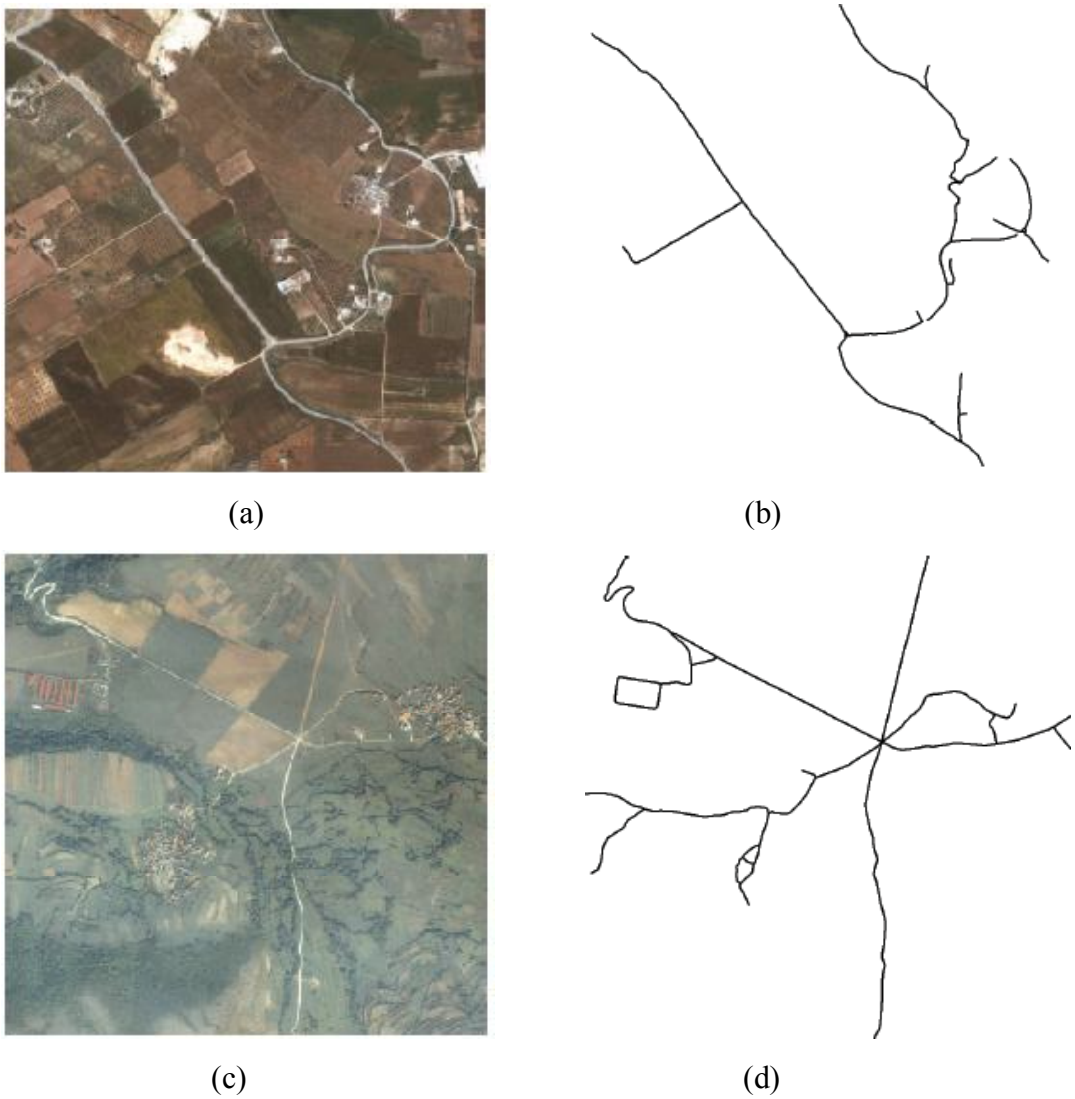

(a) (b)

(c) (d)

Figure 7: (a) Tunis Image (b) Result of automatic road extraction (c) Kosovo Image (d) Result of automatic road extraction. Courtesy of Bacher & Mayer, (2005)

2.6 Other Approaches for Road Extraction

Road tracking, pixel footprint and Fourier shape descriptor algorithms are applied for road and intersection extraction in Hu, Razdan, Femiani, Wonka, & Cui (2007). Road tracking needs a starting pixel and iteratively choose direction of another pixel

to obtain whole line segment. The problems solved are how to start road tracking and how to find toes of a footprint using Fourier shape descriptor of pixel footprint.

High resolution HYDICE images are used for road extraction in Oddo, Douccette, & Agouris (2000). In this approach a hybrid combination of self organization and model-based extraction techniques are applied. A region-based center-of-gravity approach is a cluster analysis technique to find and map spatial structure within segmented road pixels. Sample road pixels are classified using *Maximum Likelihood* (ML) spectral classifier and then *K-medians filtering* and *minimum spanning tree* methods are applied to identify general structure of road network. After that simple road segments are fitted using model based.

In Liu, Li, & Chapman , Quickbird pan-sharpened satellite images are used for road extraction (2003). *Cluster analysis*, *fuzzy-c means* and *genetic algorithms* are sequentially applied. In this approach, the human interaction is not wanted for cluster, so genetic algorithms are performed to learn parameters and pick up appropriate clusters automatically.

Like Barsi, et al. (2002) and Amini, et al. (2002), 1-meter resolution IKONOS images are used for road extraction in Yu, Lee, & Lee (2003). In this approach, road network extraction is based on *Gradient Direction Profile Algorithm* (GDPA) because of its performance and further applicability. Before GDPA, pre-processing steps that are *overall accuracy evaluation* and *ranking-error assessment* are performed. In this manner, road information can be extracted automatically.

As different from Yu, et al. (2003) IKONOS satellite images are used for road extraction using template matching technique in Kim, Park, Kim, Jeong, & Kim (2002). This approach is semi-automatic and a user's input is required. User identifies one point on a road centerline, then a template window is defined centered on the point and orientation estimation of the template is calculated. After that template

window and initial target window are obtained and least squares correlation matching is applied. These processes are iteratively applied while new road center and orientation is obtained.

The system is mainly based on human-computer interactions in Zhou, Bischof, & Caelli (2006). Because of continuous human-computer interactions, complete and right results are obtained and the performance and reliability of road tracking are optimized. This algorithm consists of Bayesian filtering, particle filter and Kalman filter that are performed with human inputs to estimate road axis points and update the tracking algorithms. Block Diagram of human-computer interaction based tracking is shown in figure 8.

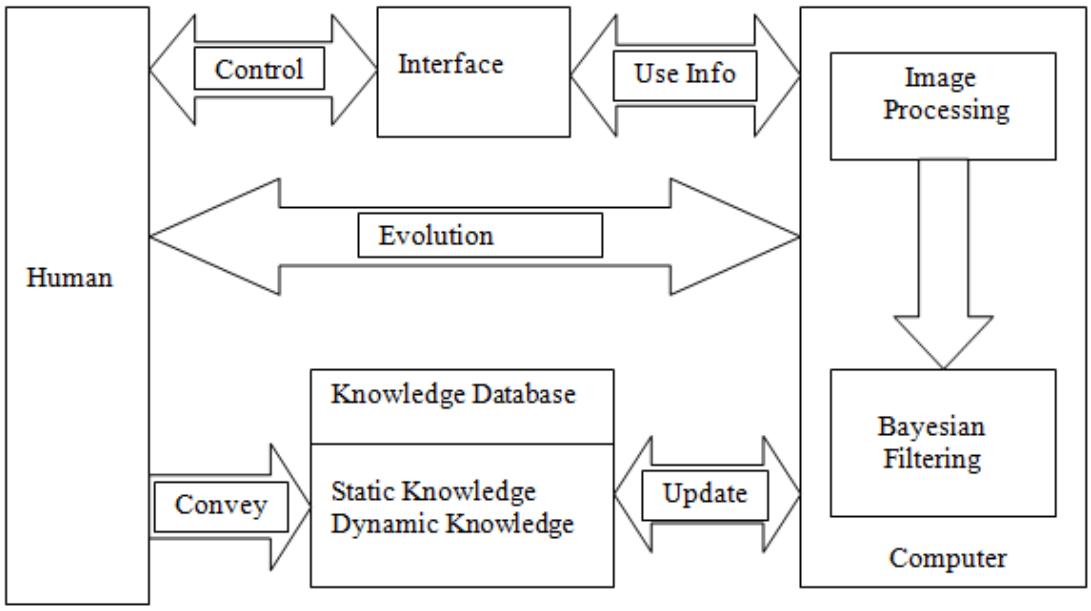

Figure 8: Block Diagram of Road Tracking System

In Gardner, Roberts, Funk, & Noronha (2001), AVIRIS data are used for road extraction. AVIRIS data provide detailed and continuous radiance information. *Spectral mixture* and *Q-Tree filter* are applied in this approach. Firstly the urban spectral library is developed by extracting and averaging 3.9 meter resolution spectra from the AVIRIS data. After that the urban materials are mapped using spectral

mixture analysis. Then Q-tree filter analysis is applied for extraction of shadowed roads by tree.

Information extraction ability of other approaches and applications such as fuzzy logic, wavelet, hough, knowledge base, canny, morphology, etc. from aerial and satellite images are examined and performances of these algorithms have been compared experimentally in the literature. On the other hand, snake algorithm is not scrutinized so much. In the past experiments, synthetic images were used quite more than real images. Thus it is hard to understand performances of snake algorithms that are ribbon and ziplock snake. However it has been shown that promising results have been acquired using snake algorithm. Therefore, we chose snake method to study in this thesis and ribbon and ziplock snake evaluate snake to methods using various images containing salient and non-salient roads.

CHAPTER 3

ROAD EXTRACTION USING SNAKES

3.1 Snakes: An Active Contour Model

Snakes that are active contour models are used to obtain object boundaries as curves using internal forces coming from the curves itself and image forces computed from the image data. For road extraction, initialization of the snake is important because the snake's position is optimized locally close to its initial position. Snakes consist of photometric and geometric constraints. The photometric constraints provide to optimize snake in respect of image feature properties. The geometric constraints consist of the elasticity and rigidity parameters of the optimizing snake. The elasticity and rigidity parameters have a great importance in the behavior of the curve.

Snakes have two representation types that are analytical and discrete representation. In the next section these types are explained.

3.2 Analytical Representation

The original snake introduced by Kass et al. is modeled as time-dependent 2-D curves with a parametric representation (1987). Snake is defined as

$$v(s,t) = \big(x(s,t), y(s,t)\big) \quad 0 < s < 1 \qquad \text{EQUATION (1)}$$

Where v is the arc, s is the length of arc, t is the time of iteration, and x and y are the coordinates of image. As time progresses, the snakes are optimized according to the

forces. These forces are image forces and internal forces. Image forces push the initial or last optimized snake toward the feature in the image. Internal forces are which control the shape of the snake to hold the curve and to keep it from bending too much, imposing piecewise smoothness. These forces are defined to optimize image as flexible and adaptively for different tasks by changing its global properties.

3.2.1 Energy of the Snake

After defining initial snake position, we optimize snake optimal position depending on an iteration time. In this step the forces are used for obtain energy as mentioned about them in chapter 2. This energy is represented as (Klang, 1998):

$$E(v) = E_{img}(v) + E_{int}(v) \qquad \text{EQUATION (2)}$$

where *E(v)* Energy of the snake is sum of the image energy and internal energy. The E_{int} represents internal energy depends on internal forces and the image energy E_{img} gives rise to the image forces (Xu & Prince, 1998). Snake's total energy E obtained, and for each iteration snake's position is defined until local minimum of E is found. The image energy is defined as

$$E_{img}(v) = \int_0^1 P\big(v(s,t)\big)\, ds \qquad \text{EQUATION (3)}$$

where $P\big(v(s,t)\big)$ is usually accepted as magnitude of the image's gradient. This is defined as,

$$P\big(v(s,t)\big) = |\Delta I(v(s,t))| \qquad \text{EQUATION (4)}$$

where $I(v(s,t))$ is the image convolved by a Gaussian kernel that is defined by the user. The Gaussian Kernel Filter smoothes the original image to remove irrelevant features as depending on chosen filter type (Neuenschwander et al. 1997) (Xu & Prince, 1998) (Neuenschwander, Fua, Szekely, & Kubler, 1995). In this situation user defined Gaussian Kernel Filter acts as an important factor to detect salient roads. Different type of Gaussian Kernel Filter cause different or most probably wrong solutions. This problem is explained in chapter 3. The internal energy (Neuenschwander, Fua, Szekely, & Kubler, 1997, December) is defined as

$$E_{int(\vec{v})} = \frac{1}{2}\int_0^1 \alpha(s)\left|\frac{\partial\vec{v}(s,t)}{\partial s}\right|^2 + \beta(s)\left|\frac{\partial^2\vec{v}(s,t)}{\partial s^2}\right|^2 ds \qquad \text{EQUATION (5)}$$

where α (alpha) and β (beta) parameters are chosen by user and indicate the snake's elasticity and rigidity. As mentioned before, the geometric constraints consist of the elasticity and rigidity parameters of the optimizing snake and these parameters influence the behavior of the curve (Mayer, Laptev, Baumgartner, & Steger, 1997). So Internal energy introduces geometric constraints on the shape of snake. The elasticity and rigidity is sequentially introduced by the first order and second order term.

3.2.2 Minimization of Snake's Energy

Energy minimization is main logic of snake for the feature extraction. Minimum energy of snake means that edge of the feature is detected and final shape of snake is created in optimization procedure. We mentioned about the formula of the snake's energy. These formulas have image energy and internal energy as explained before. Using these formulas, the snake's total energy formula is defined as (Xu & Prince, 1998):

$$E(\vec{v}) = -\int_0^1 P\big(\vec{v}(s,t)\big)ds + \frac{1}{2}\int_0^1 \alpha(s)\left|\frac{\partial \vec{v}(s,t)}{\partial s}\right|^2 + \beta(s)\left|\frac{\partial^2 \vec{v}(s,t)}{\partial s^2}\right|^2 ds$$

EQUATION (6)

According to the snake's total energy formula, Euler-Lagrange differential equation of the motion might give us a solution.

$$-\frac{\partial}{\partial s}\left(\alpha(s)\frac{\partial \vec{v}(s,t)}{\partial s}\right) + \frac{\partial^2}{\partial s^2}\left(\beta(s)\frac{\partial^2 \vec{v}(s,t)}{\partial s^2}\right) = -\nabla P\big(\vec{v}(s,t)\big)$$

EQUATION (7)

If this equation is shown as linear equation, minimization is separated into two different formula and solved independently for $x(s,t)$ and $y(s,t)$ (Henricsson & Neuenschwander, 1994).

$$-\frac{\partial}{\partial s}\left(\alpha(s)\frac{\partial x(s,t)}{\partial s}\right) + \frac{\partial^2}{\partial s^2}\left(\beta(s)\frac{\partial^2 x(s,t)}{\partial s^2}\right) = -\frac{\partial P}{\partial x}$$
$$-\frac{\partial}{\partial s}\left(\alpha(s)\frac{\partial y(s,t)}{\partial s}\right) + \frac{\partial^2}{\partial s^2}\left(\beta(s)\frac{\partial^2 y(s,t)}{\partial s^2}\right) = -\frac{\partial P}{\partial y}$$

EQUATION (8)

These equations generate unique solutions, so the values and derivatives of $x(s,t)$ and $y(s,t)$ have to be specified at $s = 0\ and\ 1$.

The balance between internal energy and image energy is important because one affects the other. This effect can cause to suppress the constraints of snake's smoothness or force the snake to ignore the image forces. This problem can be handled with internal energy control. Internal energy has α(alpha) and β(beta) parameters that control elasticity and rigidity of the snake. Elasticity and Rigidity provide balance between internal energy and image energy.

In automatic approach elasticity and rigidity parameters change depending on image or different contours of the same image. So these parameters must be obtained as automatically not manually as mentioned before. A constant factor λ is defined as (Fua, 1997)

$$\lambda = \frac{\left|\delta E_{img}(\vec{v})\right|}{\left|\delta E_{int}(\vec{v})\right|} \qquad \text{EQUATION (9)}$$

where δ is variation operator (Laptev et al. 2000). The balance between internal and image energy can be obtained by force to substitution of functions α and β for a constant factor λ that is calculated where initial snake position is close to final snake position. As a result Euler-Lagrange equation is modified as

$$\lambda\left(-\frac{\partial^2 v(s,t)}{\partial s^2} + \frac{\partial^4 v(s,t)}{\partial s^4}\right) = -\frac{\partial P}{\partial v} \qquad \text{EQUATION (10)}$$

where v stands for either for x or y.

3.3 Discrete Representation of the Snake

Computer systems perform discrete time applications. So the discrete representation of the snake is required to estimate snake position. To apply this, snake must be sampled as a polygonal curve with n vertices. The sampled snake polygon is defined as (Fua, 1997)

$$\vec{v}^{[t]} = \left\{\vec{v}_i^{[t]}\right\} = \left\{\left(x_i^{[t]}, y_i^{[t]}\right) = \left(x(i/n\,,t), y(i/n,t)\right)\right\}, \quad for\ i = 0, \ldots n-1 \qquad \text{EQUATION (11)}$$

where n is the number of pixels. And analytic equation is transformed to discrete equation as

$$\lambda\left(-\left(v_i^{[t]}\right)_{first-order}+\left(v_i^{[t]}\right)_{second-order}\right)=-P_v\,|_{\vec{v}_i^{[t-1]}} \qquad \text{EQUATION (12)}$$

where v stands either for x or y. $[t]$ shows iteration time. Equation (12) is solved for every vertex $\vec{v}_i^{[t]}, (i=0,\dots,n-1)$. $\left(v_i^{[t]}\right)_{first-order}, \left(v_i^{[t]}\right)_{second-order}$ that specify first and second order derivatives is written as (Cohen, 1991)

$$\begin{aligned}\lambda\left(-\left(v_i^{[t]}\right)_{first-order}+\left(v_i^{[t]}\right)_{second-order}\right)&\\ =-\lambda\left(v_{i-1}^{[t]}-2v_i^{[t]}+v_{i+1}^{[t]}\right)&\\ +\lambda\left(v_{i-2}^{[t]}-4v_{i-1}^{t}+6v_i^{[t]}-4v_{i+1}^{[t]}+v_{i+2}^{[t]}\right)&\\ =\lambda\left(v_{i-2}^{[t]}-5v_{i-1}^{[t]}+8v_i^{[t]}-5v_{i+1}^{[t]}+v_{i+2}^{[t]}\right)&\\ for\ i=0,\dots n-1&\end{aligned} \qquad \text{EQUATION (13)}$$

where v stands either for x or y. Since central differences are symmetric, they cannot be computed for the head vertices (i = 0, 1) and the tail vertices (i = n-2, n-1). Instead the forward and backward differences have to be used. The set of equations for all vertices build a system that can be written in matrix form as (Neuenschwander et al. 1997) (Neuenschwander et al. 1995)

$$K\cdot v^{[t]}=-P_v\,|_{v^{[t-1]}} \qquad \text{EQUATION (14)}$$

where $v^{[t]}$ stands for either $\left(x_0^{[t]},\dots,x_{n-1}^{[t]}\right)^T$ or $\left(y_0^{[t]},\dots,y_{n-1}^{[t]}\right)^T$ and K is a symmetric $(n-3)x(n+1)$ penta-diagonal matrix (Neuenschwander et al. 1997) (Leymarie & Levine, 1993)

$$K=\begin{pmatrix} c_{-1} & b_0 & a_1 & b_1 & c_1 & & & & & \\ & c_0 & b_1 & a_2 & b_2 & c_2 & & & & \\ & & c_1 & b_2 & a_3 & b_3 & c_3 & & & \\ & & & & \ddots & & & & & \\ & & & c_{n-5} & b_{n-4} & a_{n-3} & b_{n-3} & c_{n-3} & & \\ & & & & c_{n-4} & b_{n-3} & a_{n-2} & b_{n-2} & c_{n-2} & \\ & & & & & c_{n-3} & b_{n-2} & a_{n-1} & b_{n-1} & c_{n-1} \end{pmatrix} \quad \text{EQUATION (15)}$$

The matrix K is singular and cannot be inverted. So the equation (14) cannot be solved for $v[t]$ directly. a_i, b_i and c_i parameters are calculated as

$$\begin{aligned} a_i &= h^{-4}\left(\beta_{i-1} + 4\beta_i + \beta_{i+1} + h^2\alpha_i + h^2\alpha_{i+1}\right) \quad for\ 2 < i < n-2 \\ b_i &= h^{-4}\left(-2\beta_i - 2\beta_{i+1} - h^2\alpha_{i+1}\right) \quad for\ 2 < i < n-2 \\ c_i &= h^{-4}\beta_{i+1} \quad for\ 2 < i < n-2 \end{aligned} \quad \text{EQUATION (16)}$$

Where $h = 1/n$ and n is number of vertices and α and β is computed as shown in section 4.5.

This stems from the fact that the Euler-Lagrange differential equation has a unique solution with four supplied boundary conditions that are two points and their tangent vectors at each end of the snake. In traditional snake model (Kass et al. 1987) equation 2 is defined as

$$K \cdot v^{[t]} + P_v\,|_{v^{[t-1]}} = 0 \quad \text{EQUATION (17)}$$

This equation provides to the product of an iteration step using γ (viscosity term) and current snake position (Neuenschwander 1995). The resulting equation is defined as

$$(K + \gamma I) \cdot v^{[t]} = \gamma v^{[t-1]} - P_v \,|_{v^{[t-1]}} \qquad \text{EQUATION (18)}$$

This equation is iteratively solved to find snake's position with the local minimum of its energy as depending on a number of the iteration step. There is an nxn identity matrix I that contains the original image or smoothed image with Gaussian Kernel. $(K + \gamma I)$ is nonsingular. Thus it can be inverted matrix. In this situation $v^{[t]}$ matrix that defines calculated vertices can be obtained directly by solving numerically using $v^{[t-1]}$ matrix. γ is a viscosity term that is defined as

$$\gamma = \frac{\sqrt{2n}}{\Delta} \left| \frac{\partial E(\vec{v})}{\partial \vec{v}} \right| \qquad \text{EQUATION (19)}$$

Magnitude of Δ is set to a value considering the average displacement of the snake's vertices (Laptev et al. 2000). Because of the nonlinear term, we must verify that the energy has decreased from one iteration to the next. If instead, the energy has increased, the curve is reset to its previous position, the step size is decreased, and the viscosity is recomputed accordingly.

3.4 Ribbon Snake

Ribbon snake is extended by adding a width component to traditional snake and defined as

$$v(s,t) = \big(x(s,t), y(s,t), w(s,t)\big), \qquad (0 \le s \le 1) \qquad \text{EQUATION (20)}$$

where w is the half width of the ribbon snake (Laptev et al. 2000). For each slice of the ribbon snake $v(s_i, t_i)$, there are two points v_L and v_R correspond the ribbon's left and right sides as shown in Figure 9(a).

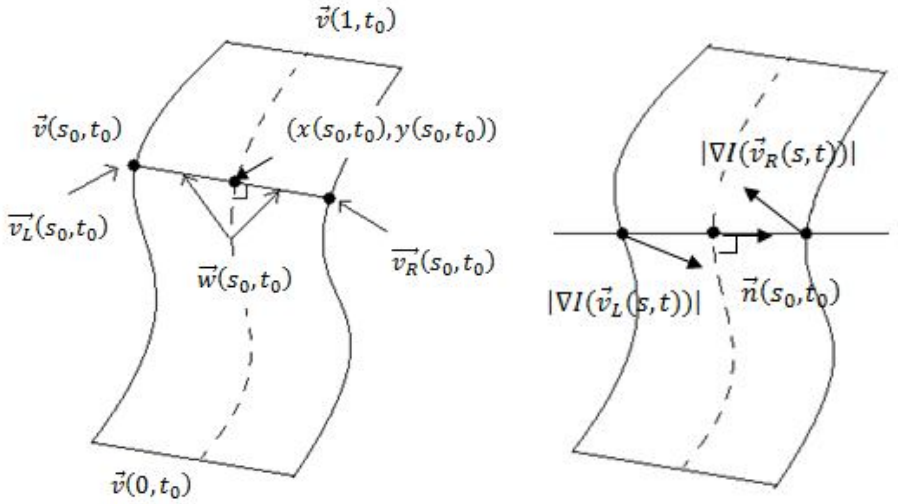

(a) (b)

Figure 9: (a) Parametric representation of the Snake (b) Image gradients and unit normal vector

The position of these boundaries can be expressed as

$$\vec{v}_R(s,t) = w(s,t) \cdot \vec{n}(s,t)$$
$$\vec{v}_L(s,t) = -w(s,t) \cdot \vec{n}(s,t) \qquad \text{EQUATION (21)}$$

where $\vec{n}(s,t)$ is ribbon's normal as shown in Figure 9(b) (Mayer et al. 1997). The unit normal vector is defined as

$$\vec{n}(s,t) = \frac{\left(\frac{\partial \vec{y}(s,t)}{\partial s}, -\frac{\partial \vec{x}(s,t)}{\partial s}\right)}{\left|\left(\frac{\partial \vec{y}(s,t)}{\partial s}, -\frac{\partial \vec{x}(s,t)}{\partial s}\right)\right|} \qquad \text{EQUATION (22)}$$

For the ribbon snake, internal energy can be directly used and the width component is constrained by same elasticity and rigidity parameters as two coordinate components. But image energy is little different from traditional snake because of the ribbon's left and right sides (Laptev et al. 2000). Image gradient magnitudes are

computed for both sides of the ribbon and they are summed to obtain P. In this way P can be defined as

$$P\big(\vec{v}(s,t)\big) = |\nabla I(\vec{v}_L(s,t))| + |\nabla I(\vec{v}_R(s,t))| \qquad \text{EQUATION (23)}$$

for both sides. While detecting the linear features that are darker or brighter than other features, the image gradients are projected onto the ribbon's normal $\vec{n}(s,t)$ to be negative along the ribbon's left side v_L and positive its right side v_R to improve the extraction result. The function P is redefined as

$$P\big(\vec{v}(s,t)\big) = |\nabla I(\vec{v}_L(s,t))| + |\nabla I(\vec{v}_R(s,t))| \cdot \vec{n}(s,t) \qquad \text{EQUATION (24)}$$

Using this equation, total energy of the ribbon snake is defined as

$$E(\vec{v}) = -\int_0^1 P\big(\vec{v}(s,t)\big)ds + \frac{1}{2}\int_0^1 \alpha(s)\left|\frac{\partial\vec{v}(s,t)}{\partial s}\right|^2 + \beta(s)\left|\frac{\partial^2\vec{v}(s,t)}{\partial s^2}\right|^2 ds \qquad \text{EQUATION (25)}$$

where first term is image energy and the second term is internal energy that is same with traditional snake internal energy equation as mentioned before (Laptev et al. 2000). The balance between image energy and internal energy is calculated like factor γ in traditional snake by equation.

During applying ribbon snake method, motion and change of the snake must be controlled. So a dissipation function D is used with the damping coefficient γ that is a viscous medium.

$$D(v) = \frac{1}{2}\int_0^1 \gamma(s)\,|v_t|^2 ds$$ EQUATION (26)

Viscous medium is similar to traditional snake viscosity term. The energy minimization equation is redefined as (Laptev et al. 2000)

$$\int \big(E(v) + D(v)\big)dt$$ EQUATION (27)

Ribbon snakes provide to extract linear features by locating their left and right boundaries.

3.5 Ziplock Snake

Ziplock snake method is developed by Neuenschwander et al. (1997). They change traditional snake discrete representation to decrease false detection range. Their method has two application parts that are initialization and optimization of snake. These steps are explained in section.

3.5.1 Initialization

Snake method is composed of initialization and optimization steps and these steps affect each other. Initialization of the snake is most important part of the snake application. As shown in figure 10, the presences of other features usually block the movement of the snake when its initial position is far away from desired result.

(a)

(b)

Figure 10: (a) Different Initializations (b) Corresponding Results. Courtesy of Neuenschwander et al. (1997)

Extended-snake based approach is developed by Neuenschwander et al. (1997) to prevent initialization and optimization problems. In extended-snake based approach, snake is initialized by end points of the snake. These end points must be clear and correct to carry out an optimization procedure correctly. The end points must have to minimum gradient value and so the system performs a linear search to find true edge location in the near neighborhood of the selected points. Starting with correctly initialized end points, optimization procedure is applied to center of the snake from end points. To achieve initialization procedure, homogeneous Euler equation is solved that it corresponds to system equation. Homogeneous Euler equation is defined as

$$-\alpha \frac{\partial^2 v(s)}{\partial s^2} + \beta \frac{\partial^4 v(s)}{\partial s^4} = 0 \qquad \text{EQUATION (28)}$$

where v stands for either x or y and $0 < s < 1$. Analytical solution of this equation is defined as

$$v(s) = C_1 + C_2 s + C_3 e^{-\sqrt{\frac{\alpha}{\beta}}s} + C_4 e^{+\sqrt{\frac{\alpha}{\beta}}s} \qquad \text{EQUATION (29)}$$

where C_1, C_2, C_3 and C_4 are integration constants that can be determined from the four boundary conditions $\{v(0), v(1), v'(0), v'(1)\}$ as two end points and their tangent values (Neuenschwander, Fua, Szekely, & Kubler, 1995). For the correct initialization procedure the other interpolation techniques are can be applied such as Bezier Curves.

3.5.2 Optimization

Optimization of the snake starts using initial snake that is defined by initialization procedure. In the optimization procedure the Ziplock snake is divided into three parts by two force boundaries (Neuenschwander et al. 1997) (Hinz, Toennies, Grohmann, & Pohle, 2001). These parts are two active parts and one passive part as shown in figure 11.

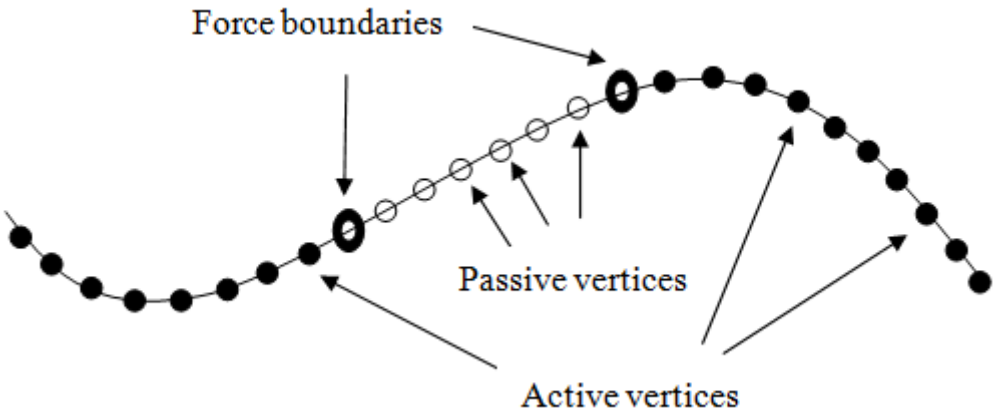

Figure 11: Active and Passive Parts of a Ziplock Snake

At the beginning of the optimization, end points are force boundaries and these force boundaries are moved towards the center of snake. For each detected force boundary, passive part of the snake is recomputed by using these new force boundaries and homogeneous Euler equation or Bezier Curves (Neuenschwander et al. 1997) and active parts are optimized to image features as shown in figure 12. The circles indicate the movement of the force boundaries during optimization.

Figure 12: Evolution of Ziplock Snake. Courtesy of Neuenschwander et al. (1997)

During optimization procedure the modified equation

$$\left(K^* + \gamma^{[t]} I\right) \cdot v^{*[t]} = \gamma^{[t]} v *^{[t-1]} - 1|_{\gamma^{[t-1]}} \cdot F^*_{v^{*[t-1]}} \qquad \text{EQUATION (30)}$$

is iteratively solved for the active vertices. γ is a similar viscosity term of traditional snake. It is initialized as $\gamma(s,0) \equiv 0, s \in [0,1]$and for each new active part is recomputed by traditional viscosity term equation that is defined before. F_v is called as the potential force field and it is defined as

$$F^*_{v^{*[t-1]}} = \begin{cases} -\dfrac{\partial P}{\partial x}|_{(x^{*[t-1]}, y^{*[t-1]})} & if\ v = x \\ -\dfrac{\partial P}{\partial y}|_{(x^{*[t-1]}, y^{*[t-1]})} & if\ v = y \end{cases} \qquad \text{EQUATION (31)}$$

The result of F_v is used to decide if the pixel is vertex or not (Neuenschwander et al. 1997). 1 is an indicator function for the vector γ and defined as

$$1|_{\gamma^{[t]}} \in IR^{(n-4)x(n-4)}\ with \quad 1_{ii} = \begin{cases} 1\ if\ \gamma_i^{[t]} > 0 \\ 0\ otherwise \end{cases} \qquad \text{EQUATION (32)}$$

$$1_{ij} = 0\ for\ i \neq j$$

This has the form of a diagonal matrix. Applying optimization formula, each force boundary is moved individually as at most one vertex per iteration step. These force boundaries provide the optimizations of new active vertices are close to previously extracted contour. As mentioned before force boundaries meet at center of the snake

but actually the optimization procedure does not stop. When they meet at center of the snake, all vertices are active. And then viscosity term is doubled for each vertex at every 10^{th} iteration until the average motion of the whole snake falls below 1/10 pixel. When this rule is provided the optimization procedure is stopped.

3.6 Road Extraction

In this thesis, road extraction is divided into three parts as salient road extraction, non-salient road extraction and crossing extraction. Salient roads are found using Ribbon Snake method. Then Ziplock snake method is applied for incomplete roads. These roads are non-salient probably and Ribbon snake method can not obtain these types of roads. These parts are explained using described methods, below.

3.6.1 Salient Road Extraction

Salient Roads are roads that are not affected or prevented by shadows or occlusions of buildings and trees. Extraction of salient roads is started with the detection of lines at a coarse scale. In this step some irrelevant lines can be detected so some rules are used to separate them as shown in figure 13. First of all, length of the roads must be restricted by a particular threshold value. If the detected line is smaller than this threshold value, it must be eliminated from extraction algorithm. Secondly to verify the roads, the precise width of the roads must be decided corresponding to the line at a coarse scale. At a fine scale while extraction, irrelevant structures having a width that is more unstable having a varying width along the line than the width of the roads are eliminated (Laptev et al. 2000).

At a coarse scale a ribbon is initialized with zero width. After that the ribbon snake algorithm is applied until the road is extracted (Laptev et al. 2000). Ribbon snake algorithm is explained in section 3.4.

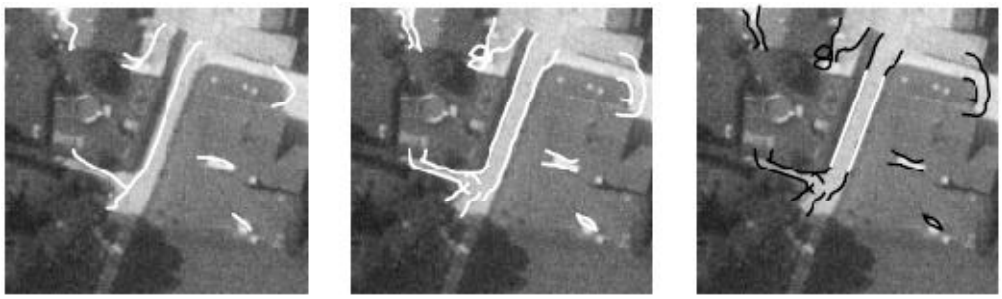

(a) *(b)* *(c)*

Figure 13: (a) Extraction of the lines (b) The optimization of the Ribbon Snake (c) Selection of the Ribbon Parts with constant width. Courtesy of Laptev et al. (2000)

In this study, Ribbon snake is experimented along whole initial snake as mentioned in section 3.4. Elimination of irrelevant features is based on length of snake. In these experiments, Ribbon snake is applied for not only salient roads but also non-salient roads and Ribbon snake method has found non-salient roads. Ribbon Snake fails to detect the part of the road covered with other features. This is due to edge detection algorithm not being able to identify the initial position of snake properly. Besides these, elasticity and rigidity parameters have been made adaptive to the image properties. These experiments were explained in chapter 4.

3.6.2 Non-Salient Road Extraction

Typical reasons of non salient roads are shadows, building, tree etc. To prevent incomplete road detection, ziplock snake is used (Neuenschwander et al. 1997). As mentioned before, ziplock snake needs two end points to initialize a snake and in the literature these end points are defined by user. Because the system is automatic, two points must be detected automatically and not defined by user. In this step ribbon snake algorithm solutions are important for non salient roads extraction. After applying ribbon snake, salient roads are extracted and these roads' start and end points can be used as ziplock snake end points. As shown in figure 14, salient roads extraction result with ribbon snake provides end points and a search space for ziplock snake to extract non salient roads.

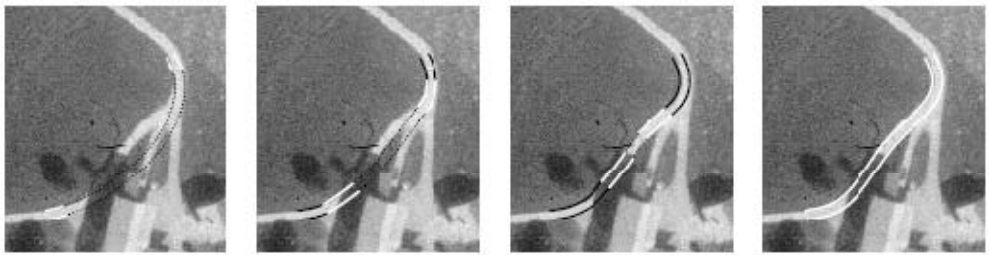

Figure 14: Initialization and Optimization steps of Ziplock Snake. Courtesy of Neuenschwander et al. (1997)

Ziplock snake algorithm is explained in section 3.5. On the other hand, Ziplock Snake method might need new control points during optimization step. This causes semi-automatic approach. Ziplock snake method is applied for both salient and non-salient roads. Besides these, optimal size of Gaussian Kernel Filter is found, because size of Gaussian Kernel Filter affects the results of Ziplock Snake. These experiments were explained in chapter 4.

3.6.3 Crossing Extraction

Extractions of salient and non-salient roads provide not only minimum search space for the crossing but also they give some initial points to detect the crossing. We can use extracted roads to find crossings. First of all, we search incomplete roads because these roads must have crossings. After that center point of the end of the incomplete road is found as shown in figure 15(a). Junctions are adjacent with previously extracted roads. Then the crossings are approximated by optimizing closed snakes around the junctions. Finally connections between the crossings and adjacent ends of previously extracted roads are obtained as shown in figure 15(d).

According to our experiments, the results of salient roads extraction are not sufficient for extraction of crossings. So we suggest new approach for extraction of crossing in chapter 4.

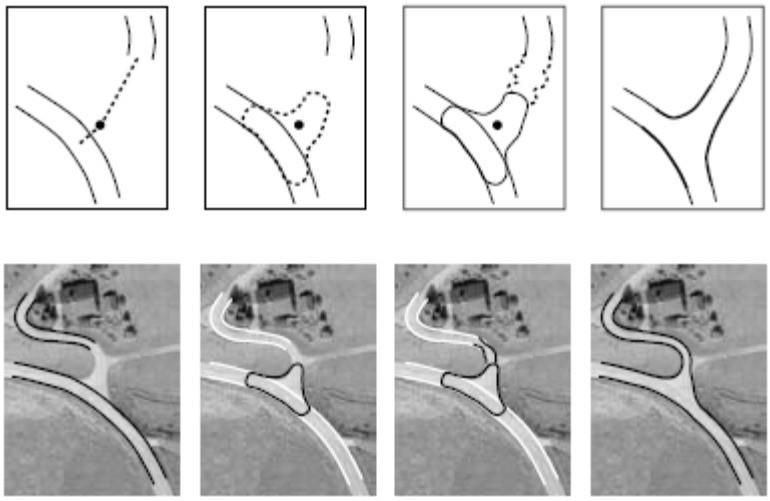

(a) (b) (c) (d)

Figure 15: Extraction of crossings. (a) Selection of initial hypothesis. (b) Approximation of the outline of the crossing. (c) Verification of connections to adjacent roads. (d) Construction and connection of the crossing. Courtesy of Laptev et al. (2000)

CHAPTER 4

EXPERIMENTAL RESULTS

In this chapter, the experimental test results of Ribbon Snake, Ziplock Snake and Crossing algorithms are discussed. Ribbon Snake and Ziplock Snake methods are compared for extraction of salient and non-salient roads. The images that have different size and resolutions are used during the experiments. Also some constant variables of these algorithms have been made adaptive according to the image properties. The images were taken from Google Maps and all results are presented by calculating the correctness and completeness of extraction. In this study, all experimented gray level images are captured from Google Maps. They have 1-meter resolution. Especially high resolutions images are preferred because their geometric properties and characteristics are discovered easily.

4.1 Ribbon Snake

Ribbon snake method is defined for salient roads extraction in Laptev et al. (2000). This algorithm is explained in chapter 3. Salient Road Extraction Flow is shown in figure 16. As shown in this figure, image must be a gray level image so real colored images are converted to the gray level images as pre-processing. The monochrome luminance is calculated by combining the RGB (Red, Green, and Blue) values according to the NTSC (National Television System Committee) standard, which applies coefficients related to the eye's sensitivity to RGB colors. Equation of this method is defined as

$$I = 0.2989 * R + 0.5870 * G + 0.1140 * B \qquad \text{EQUATION (33)}$$

where R, G and B represent the Red, Green and Blue values respectively and *I* is an intensity image with integer values ranging from a minimum of 0 to maximum of 255.

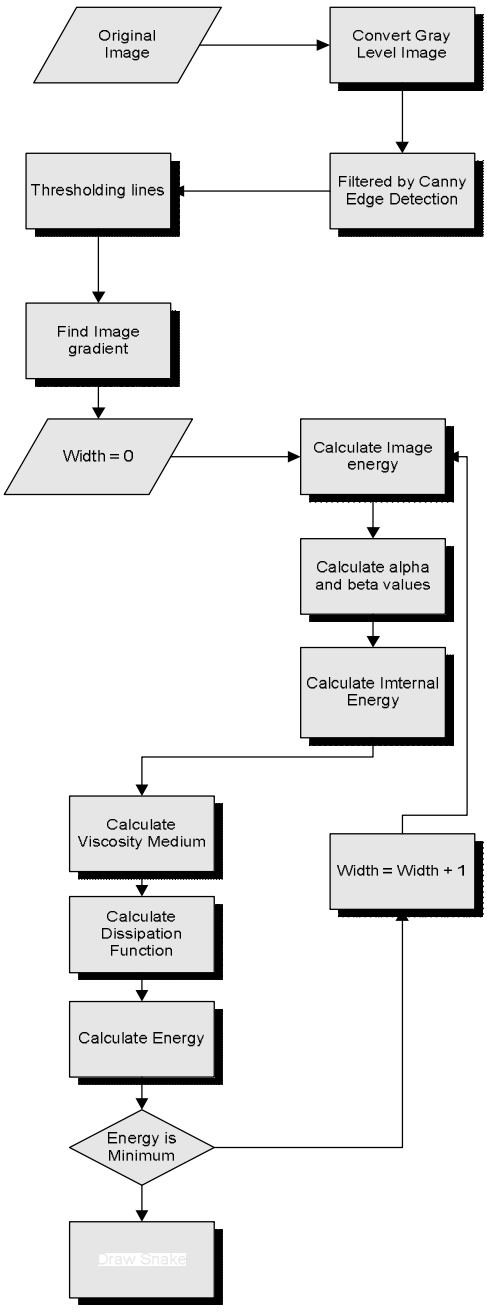

Figure 16: Ribbon Snake Flow Diagram

In the experiments, Ribbon Snake initialization is important. In Kass et al. (1987), initial snake position is defined by the user as semi-automatic feature extraction. In this model, initial position of the snake is defined by using the Canny edge detection filter automatically. After the edge detection step, if detected lines are smaller than the defined threshold value of length, they must be eliminated while applying the extraction algorithm. Threshold value is selected as 15 pixels. As shown in figure 17, initial snake position is detected by eliminating irrelevant lines.

Figure 17: Initial Snake

During Ribbon snake application, initial snake position is moved towards ribbon snake's left and right. The equations are defined for this motion as

$$x_{left/right} = x_{current} \pm w_t * \cos(\tan^{-1} x_{current})$$
$$y_{left/right} = y_{current} \pm w_t * \sin(\tan^{-1} y_{current}) \quad \text{EQUATION (34)}$$

where $x_{left/right}$ and $y_{left/right}$ are the ribbon snake's left and right x and y. $x_{current}$ and $y_{current}$ are the ribbon snake's current x and y. w_t is the half width of

the snake and t is the iteration number. Then, the total energy is calculated by using equation (28) for new snake. Number of iterations is taken as 50.

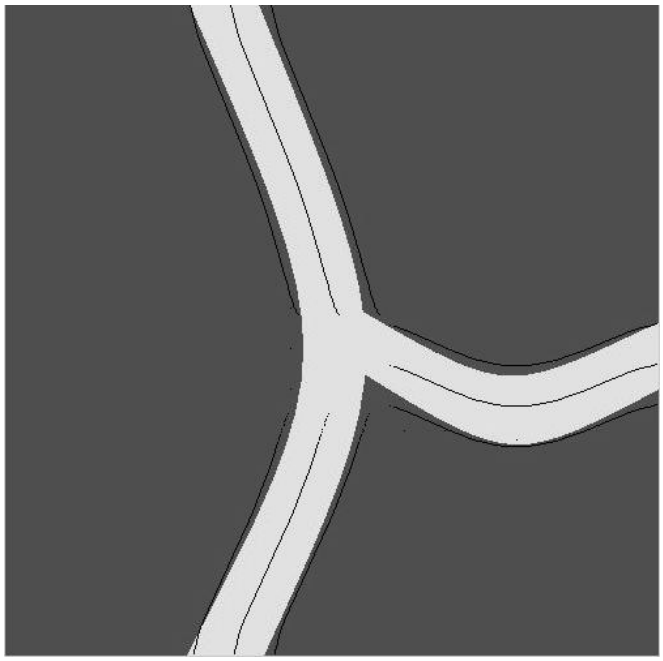

Figure 18: Initial snake and detected roads in a synthetic image

After all iterations are completed, the half width that has the minimum total energy is established. As shown in figure 19, road lines are obtained by using equation (34), half width and initial position of ribbon snake in figure 17, and process stops. Another example is shown in figure 18. This image is a synthetic image. For this synthetic image, elapsed time of all processes is fewer than real images.

Detection results are shown in figure 20 for different images and the results are evaluated. Table 1 shows the evaluation of salient roads extraction using Ribbon Snake. Correctness describes the percentage of the detected road pixels in a result of an extraction. For example, the correctness of figure 19 shows that the result of extraction has 77.58 percent of road pixels and %22.42 percent of non-road pixels. Completeness describes the percentage of the road pixels that were detected in an image as all the pixels are inside the detected road area. For example, the

completeness of figure 19 shows that result of extraction has 100 percent of road pixels in the image. According to the results, Ribbon snake detects 86.74 percent of salient road pixels on average for these test images.

Figure 19: Detected road lines using Ribbon Snake

Table 1: Evaluation of results for Salient Roads Using Ribbon Snake

	Figure 18	Figure 19	Figure 20(a)	Figure 20(b)	Figure 20(c)	Average
Correctness	%90.87	%77.58	%92.48	%83.55	%89.21	%86.74
Completeness	%98.47	%100	%100	%100	%99.02	%99.50
Image Size (pixel)	348x434	350x301	344x350	221x116	503x504	

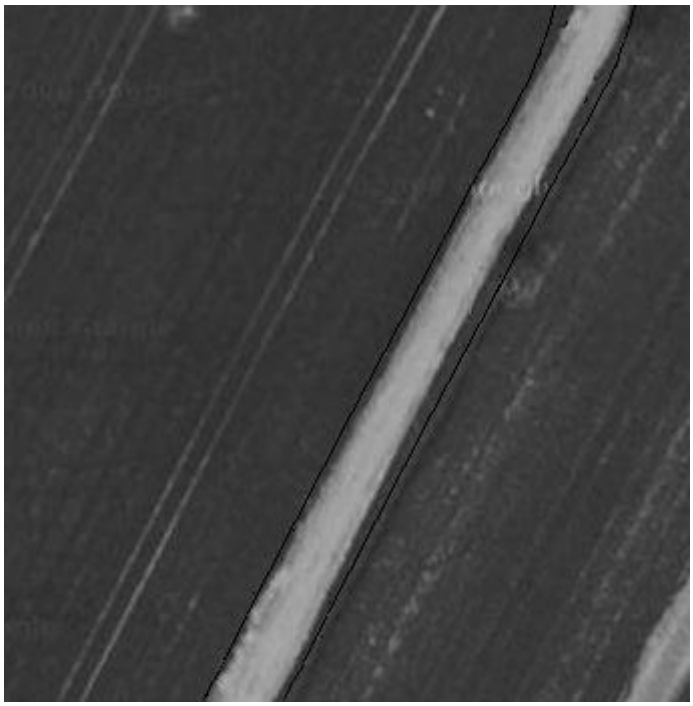

(a)

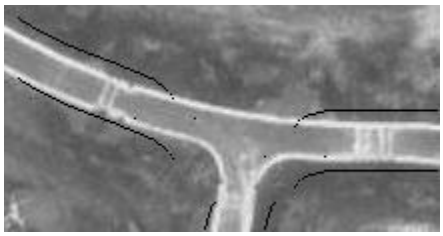

(b)

(c)

Figure 20: (a), (b) and (c) Other Detected road lines using Ribbon Snake

Ribbon snake algorithm is defined and performed for salient road in the literature as mentioned above. Ribbon Snake has also been applied for non-salient roads in this thesis. Figure 21 and 22 show results of non-salient road extraction using Ribbon Snake. Figure 21 is a 1-meter resolution synthetic image that is manually shaded. On the other hand figure 22 is a 1-meter resolution test image which has real shadows.

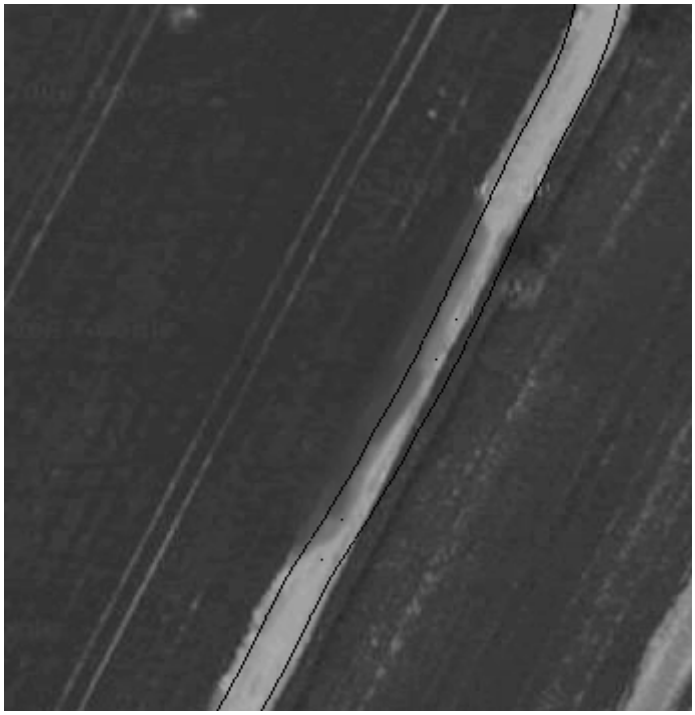

Figure 21: Result of Non-Salient road extraction

Table 2 shows evaluation of non-salient roads extraction using Ribbon Snake. Contrary to mentioned in literature, depending on initialization step of Ribbon Snake in complex image, extraction of non-salient roads can be performed by using Ribbon Snake algorithm. Because, in complex images, initialization step of Ribbon snake might not be performed by using canny edge detector correctly. The results show that correctness and completeness of Ribbon Snake algorithm are 93.59 percent and 87.98 percent on an average respectively.

Table 2: Evaluation of results for Non-Salient Roads Using Ribbon Snake

	Figure 21	**Figure 22**	**Average**
Correctness	%100	%87.016	%93.59
Completeness	%75.962	%100	%87.98
Image Size (pixel)	344x355	497x433	

Figure 22: Detected non-salient road lines using Ribbon Snake

On the other hand, the detection might fail, because of the wrong elasticity and rigidity parameters, and initialization. Elasticity and rigidity parameters manually defined by user might cause incorrect extraction of roads in an image. Besides this, proper initialization of ribbon snake is an important factor affecting the results significantly. Canny filter is not sufficient to detect line in the complex images. Thus

if initialization step is performed as inadequate, energy minimization formula is applied for wrongly initialized snake positions as shown in figure 23. In this experiment, elasticity and rigidity parameters were taken as 0.3 and 0.5. Because of chosen random elasticity and rigidity parameters, energy minimization formula was failed on detection of roads.

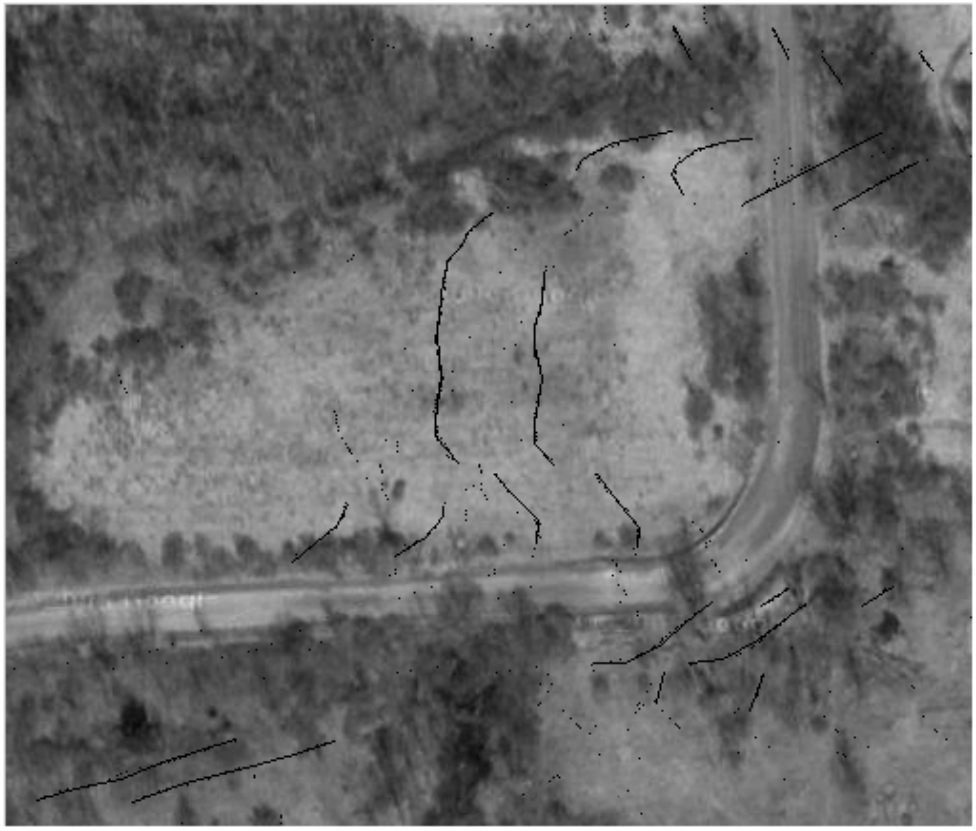

Figure 23: Failed detection using Ribbon Snake

Ribbon snake can be initialized using any edge detection algorithm but features like roads affect this step's accuracy. Ribbon snake uses all this extracted information regardless of the features being irrelevant. Even if minimization algorithm is executed correctly, incorrect initialization causes failure in detection of roads.

In detection of non-salient roads, shadows result in incorrect width estimation due to minimum energy being found near the shadow edges. We can increase or decrease

number of iterations or threshold value of minimum energy to prevent this problem. However these changes can decrease completeness of road extraction.

4.2 Ziplock Snake

Ziplock snake method is developed by changing discrete representation of the traditional snake to decrease false detection range. The method has two application parts that are initialization and optimization of snake. Before these steps, pre-processing step is applied as shown in figure 24. This step consists of smoothing of image with Gaussian Kernel Filter. Although importance of the size of Gaussian Kernel Filter is not mentioned in the literature, different sizes of Gaussian Kernel Filter give different results. Thus, optimal size of Gaussian Kernel Filter is found as mentioned below.

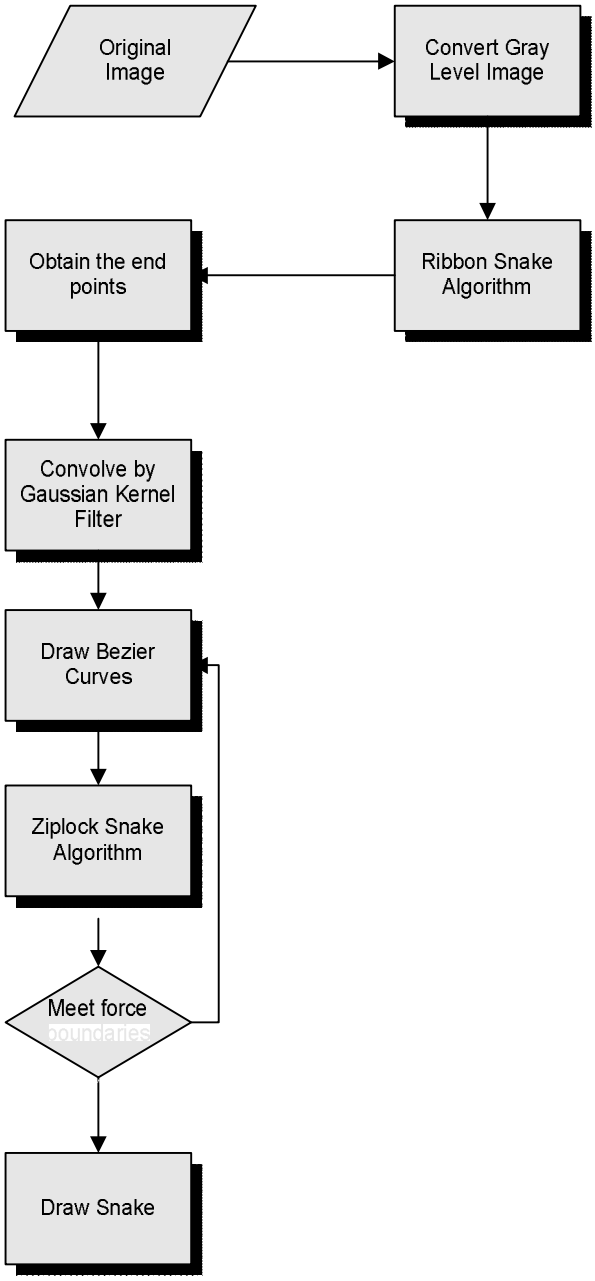

Figure 24: Ziplock Snake Flow Diagram

4.2.1 Experiments of Gaussian Kernel Filters

During the experiments, Gaussian Kernel Filters in size of (10x10), (20x20), (30x30), (40x40) and (50x50) have been tried. Figure 25 shows the results of

extraction using Gaussian Kernel Filter in size of (10x10), (20x20), (30x30), (40x40) and (50x50) and table 3 shows numerical results. Depending on these experiments, Gaussian Kernel Filter in size of 30x30 gives 88.57 percent extraction of road pixels in 1-meter resolution image that is shown in Figure 25(c). This result is the best as shown in the table 3. On the other hand, if the size of Gaussian Kernel Filter is increased or decreased, correctness decays as shown in figure 25(a), (b) and (d).

Table 3: Evaluation of Different Size of Gaussian Kernel Filter

	Gaussian Kernel (10x10) Figure 25(a)	**Gaussian Kernel (20x20) Figure 25(b)**	**Gaussian Kernel (30x30) Figure 25(c)**	**Gaussian Kernel (40x40) Figure 25(d)**	**Gaussian Kernel (50x50) Figure 25(e)**
Correctness	%83.87	%82.99	%88.57	%73.33	%65.56
Completeness	%95.47	%94.36	%97.35	%98.53	%97.77
Image Size (pixel)	348x434	342x434	342x434	342x434	342x434

Because the iteration time is quite long, some ranges of size of Gaussian Kernel Filter are tested. Certain Gaussian blurring helps to detection, but excessive blurring causes to disappear of features. Therefore performance of extraction decreases.

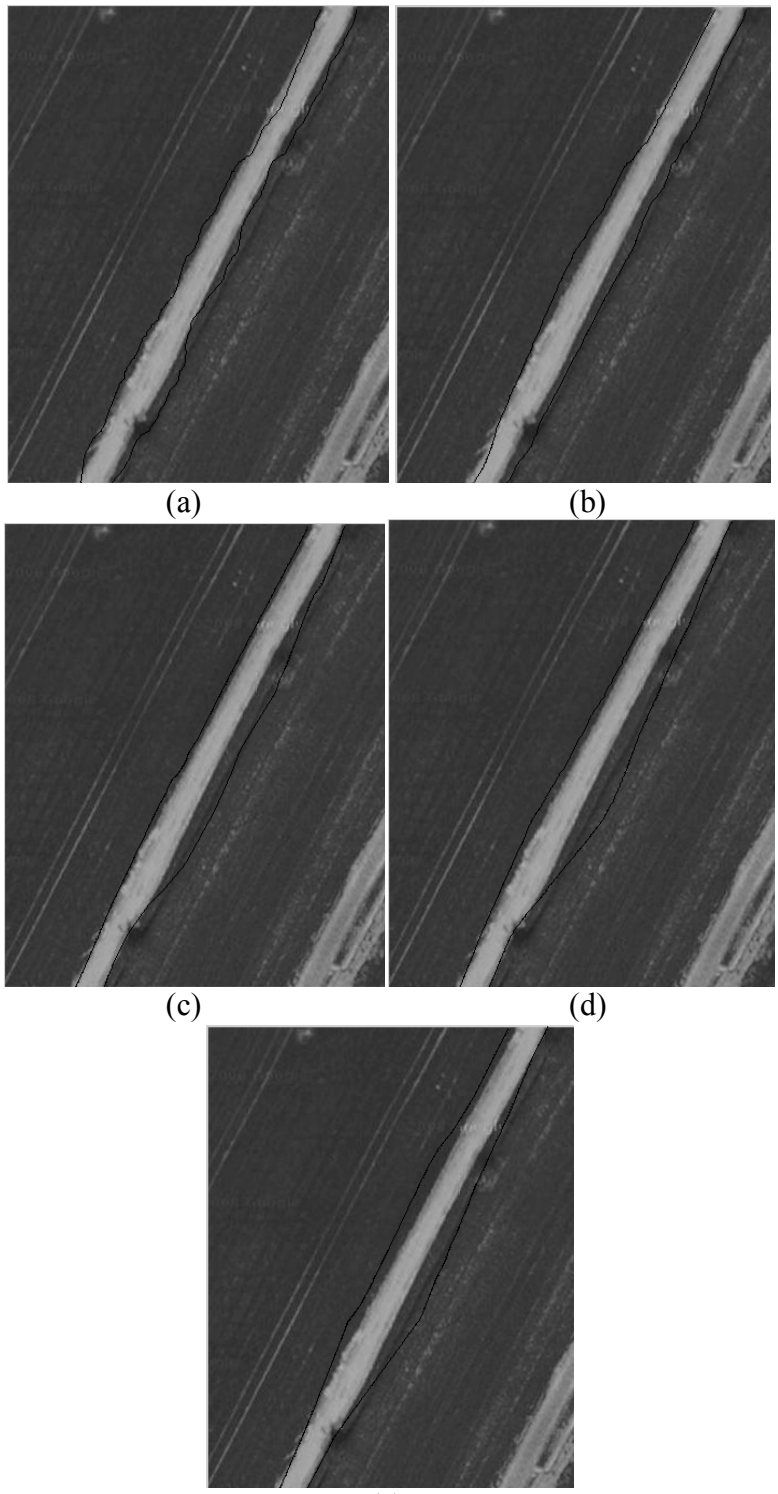

Figure 25: (a)Ziplock Snake (10x10) Gaussian Kernel Filter (b)Ziplock Snake (20x20) Gaussian Kernel Filter (c)Ziplock Snake (30x30) Gaussian Kernel Filter (d)Ziplock Snake (40x40) Gaussian Kernel Filter (e)Ziplock Snake (50x50) Gaussian Kernel Filter

In addition, optimal Gaussian Kernel Filter size depends on the resolution of the image. According to the experiments, if resolution of an image is changed, size of the Gaussian Kernel Filter must be changed by approximately the same ratio. Figure 25(c) and 30 are converted from 1-meter resolution images to 2-meter resolution images using *pyramidal decomposition*. After that, Gaussian Kernel Filter in size of (15x15) and (10x10) is applied as pre-process for these low resolution images. Figure 26 and 31 show results of road extraction algorithm. Depending on these figures, table 4 and table 5 are generated. While correctness and completeness are 55.83 percent and 100 percent respectively for 1-meter resolution image that is shown in figure 30, these percentages are 57.24 and 100 respectively for 2-meter resolution image that is shown in figure 31(a). And also figure 25(c) and figure 26(a) give similar results. On the other hand, Gaussian Kernel filter in size of (10x10) gives worse result than (15x15) for 2-meter resolution images. According to these results, if resolution is decrease or increase, size of Gaussian kernel filter might be changed as same ratio with resolution change.

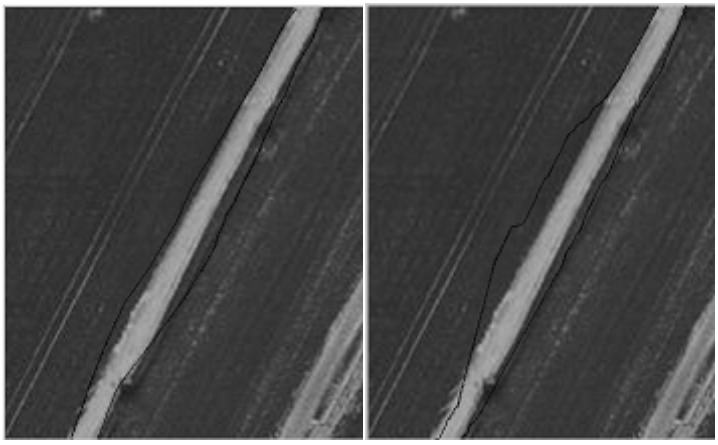

(a) (b)

Figure 26: (a) Ziplock Snake with (15x15) Gaussian Kernel Filter (b) Ziplock Snake with (10x10) Gaussian Kernel Filter

Table 4: Evaluation of Different Size of Gaussian Kernel Filter for image in figure 25(c) and down sampled version in figure 26

	Gaussian Kernel Filter (30x30) Figure 25(c)	Gaussian Kernel Filter (15x15) Figure 26(a)	Gaussian Kernel Filter (10x10) Figure 26(b)
Correctness	%88.57	%85.53	%63.13
Completeness	%97.74	%97.77	%98.11
Image Size (pixel)	347x435	173x217	173x217

Table 5: Evaluation of Different Size of Gaussian Kernel Filter for image in figure 30 and down sampled version in figure 31

	Gaussian Kernel Filter (30x30) Figure 30	Gaussian Kernel Filter (15x15) Figure 31(a)	Gaussian Kernel Filter (10x10) Figure 31(b)
Correctness	%55.83	%57.24	%47.53
Completeness	%100	%100	%57.33
Image Size (pixel)	513x437	257x218	257x218

4.2.2 Experiments of Initialization and Optimization Steps

The next step after the pre-processing is initialization. This step is performed by using Bezier Curves as shown in Figure 27. Bezier Curves are generated between the end points. The end points must have minimum gradient value. Thus the system performs a linear search to find true end points in the neighborhood of the selected end points. And then optimization procedure is applied from the correct end points to center of the snake. At the beginning of the optimization, end points are force boundaries and these force boundaries are moved towards the center of snake. As mentioned in chapter 3, during optimization procedure the modified equation (31) is iteratively solved for the active vertices.

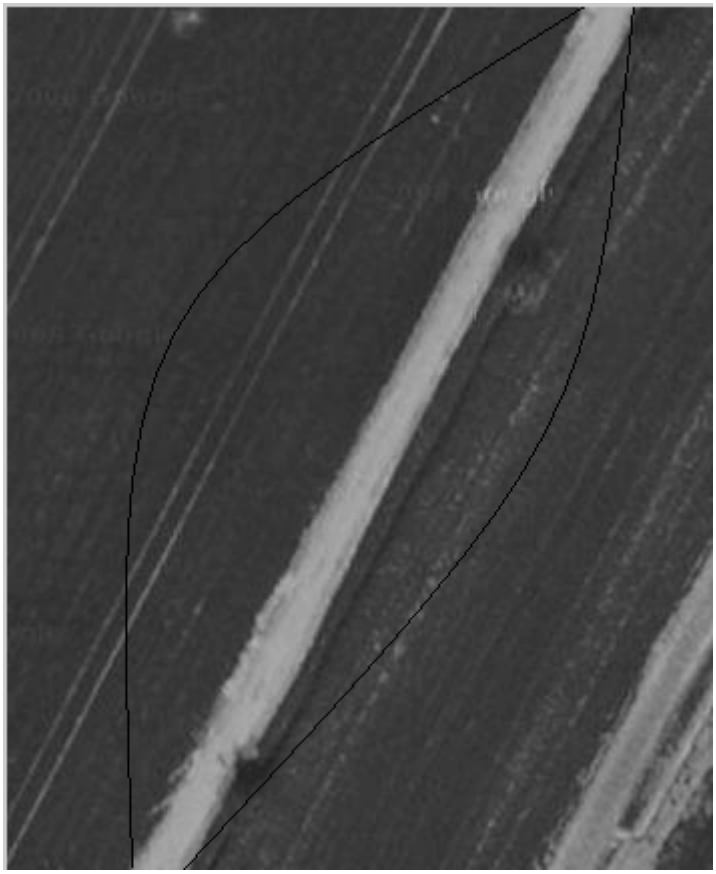

Figure 27: Bezier Curves

At the end of the each iteration, two new force boundaries are formed. Then, passive part of the snake is recomputed by using these new force boundaries and Bezier Curves.

When force boundaries meet at the center of the snake, the optimization procedure does not stop. In this situation, all vertices are active. The viscosity term that is defined in equation (20) is doubled for each active vertex at every 10^{th} iteration until the average motion of the whole snake falls below 1/10 pixel. When this rule is provided, the optimization procedure stops.

According to the experiments, Ziplock snake detects straight roads, while it is not successful in detecting curved roads as shown in Figure 28. Ziplock snake needs

some new control points that are defined by user during optimization. For an automatic approach, this situation is not appropriate. Thus, Ziplock snake is not capable of curved road detection automatically. Depending on the results of extraction in table 6, while correctness and completeness are 83.45% and 100 % for figure 28, correctness are 88.57 percent and completeness is 97.74 percent for figure 25(c). As a consequence, if images that have straight roads are chosen, success of Ziplock snake method increases for automatic approaches.

Figure 28: Detected roads using Ziplock Snake

According to the literature, the implementation area of Ziplock Snake consists of non-salient roads, indeed. As shown in figure 29, Ziplock Snake detect roads for a simple image that is modified by user to generate synthetic shadows. On the other hand, Ziplock Snake is incompetent for real images that have non-salient roads. Depending on the evaluation of the results in table 7, correctness is 55.83 percent of non-salient roads and completeness is 100 percent using Ziplock Snake method for real image as shown in Figure 30. As mentioned above, Ziplock Snake is not sufficient for extraction of roads in complex images and needs new control points

that are defined by users during iterations. But this situation is adverse to the automatic approach logic. Besides this, correctness is 72.43 percent of non-salient roads and completeness is 98.79 percent using Ziplock Snake method for modified image as shown in Figure 29. This rise of correctness depends on image and road properties.

Table 6: Evaluation of Ziplock Snake for salient roads

	Figure 25(c) (salient)	**Figure 28 (salient)**	**Average**
Correctness	%88.57	%83.45	%86.01
Completeness	%97.74	%100	%98.87
Image Size (pixel)	347x435	349x303	

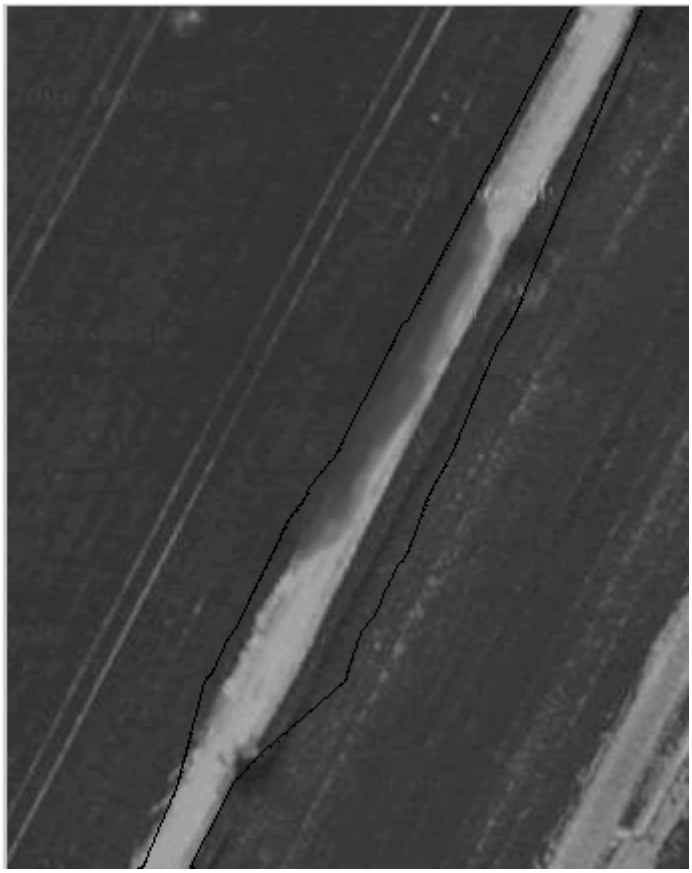

Figure 29: Detection of roads for simple image that is modified by user using Ziplock Snake

Figure 30: Ziplock Snake with Gaussian Kernel (30x30)

(a) *(b)*

Figure 31:(a) Ziplock Snake with Gaussian Kernel (15x15) (b) Ziplock Snake with Gaussian Kernel (10x10)

Table 7 : Evaluation of Ziplock Snake for non-salient roads

	Figure 29 (non-salient)	**Figure 30 (non-salient)**	**Average**
Correctness	%72.43	%55.83	%64.13
Completeness	%98.79	%99.13	%98.96
Image Size (pixel)	344x434	513x437	

A failure case is shown in figure 32. Causes of failure in this experiment are; using unsuitable Gaussian kernel filter, manual representation of elasticity and rigidity parameters, and similar geographic properties of roads and other features. Elasticity and Rigidity parameters refer to alpha and beta parameters. Their calculation is defined in section 4.5. But alpha and beta parameters are chosen randomly as 0.3 and 0.5 in this experiment. On the other hand magnitudes of gradient values of the pixels may be similar. Besides this, chosen Bezier curve is effect the result. Because any new control number can not be defined manually for an automatic road extraction, length of Bezier curves must be described as conceivable.

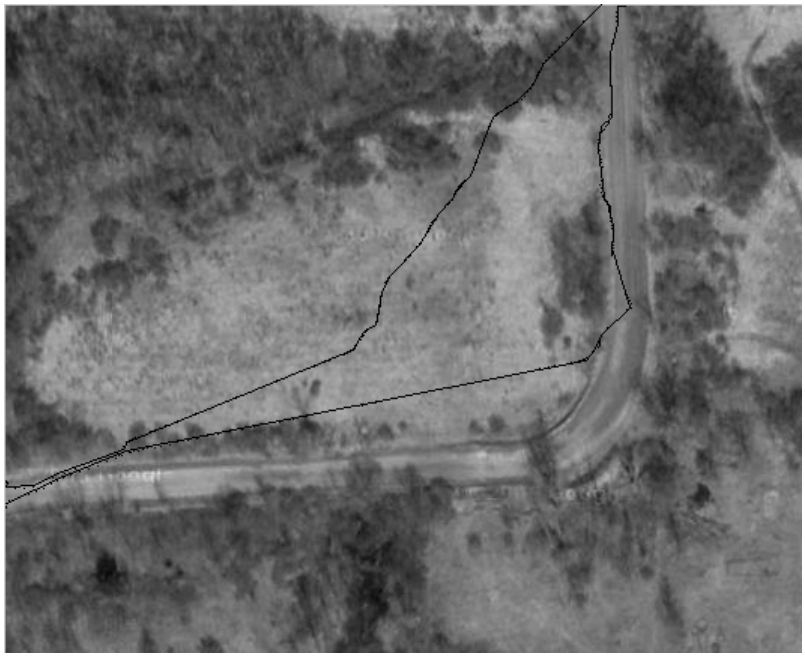

Figure 32: Failed detection using Ziplock Snake

Ziplock snake needs initial end points and this algorithm is applied between these end points. During optimization procedure, new force boundaries are obtained and force boundaries meet at the center of the snake as mentioned before. Number of iterations is generally around 1500-3000. We can change the parameters of Ziplock snake that are Gaussian kernel filter size, viscosity term and the average motion of whole snake. But these changes cause decreases in both correctness and completeness for extraction.

4.3 Non-salient Road Extraction with Ribbon Snake and Ziplock Snake

Non-salient roads can be detected by using Ribbon Snake and Ziplock Snake together. If Ribbon Snake does not extract all roads in an image, Ziplock Snake completes undetected roads using the end points of detected roads. As described above, Ribbon snake was executed for non-salient roads too. In these experiments Ribbon snake did not need Ziplock snake method and could find non-salient roads. On the other hand, figure 33 shows detection of roads using Ribbon Snake and Ziplock Snake together.

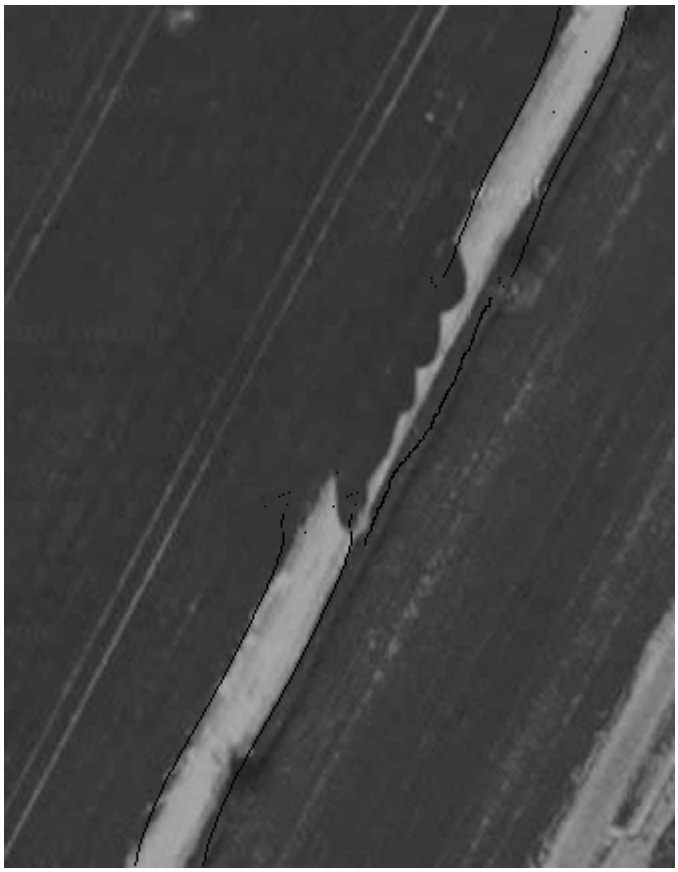

Figure 33: Extraction of Road Using Ribbon Snake and Ziplock Snake

In this experiment, Ribbon Snake fails to detect the part of the road covered with other features. This is due to edge detection algorithm not being able to identify the initial position of snake properly. As a result Ribbon Snake algorithm can not perform extraction for whole roads. Besides this, Ziplock snake method was implemented for only uncovered edge.

4.4 Comparison Between Ribbon Snake and Ziplock Snake Methods

In this part, results of Ribbon Snake and Ziplock Snake algorithms were compared and evaluation tables were constituted.

Table 8: The results of extraction of salient roads

	Ribbon Snake	**Ziplock Snake**
Correctness	%85.71	%84.51
Completeness	%99.90	%98.87

According to the table 8 Ribbon snake and Ziplock snake gives similar results for extraction of salient roads. But as shown in table 9, the results of ribbon snake and ziplock snake method are quite different for extraction of non-salient roads. Ziplock snake have much more low percentage than Ribbon snake at extraction of non-salient roads. Because of this, as mentioned above, Ziplock snake must be initialized by using more than two end points. In this manner, Ziplock snake success can be increased by using these points. Beside this, Ziplock snake might need new control points during optimization. On the contrast, Ribbon snake does not need any user intervention. Ziplock snake initialization step requires end points that are defined by output of the Ribbon snake method or users. On the other hand, Ribbon snake method requires only right initialization using any edge detection method.

Table 9: The results of extraction of non-salient roads

	Ribbon Snake	**Ziplock Snake**
Correctness	%93.51	%66.13
Completeness	%87.98	%98.96

4.5 Alpha (α) and Beta (β) Parameters

α (alpha) and β (beta) parameters have been described as constant in Laptev et al. (2000). According to the failure experiments of Ribbon snake and Ziplock snake methods shown above, alpha and beta parameters must not be constant and defined by user. In an automatic approach, elasticity and rigidity parameters change depending on the original image or different contours of the same image. As

mentioned in chapter 2, a constant factor λ may be defined by using equation (9). In this equation, δ (sigma) is variation operator.

The balance between internal and image energy can be obtained by force to substitution of functions α and β for a constant factor λ that is calculated where initial snake position is close to final snake position.

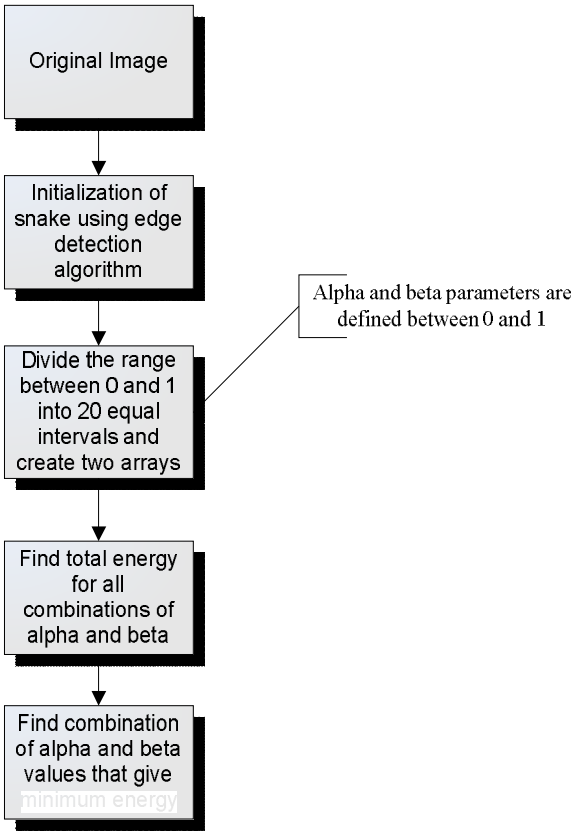

Figure 34: Calculation of Elasticity and Rigidity Parameters Flow Diagram

In this situation, there is not only a δ variation operator but also α and β parameters that must be found for whole process. Therefore, α and β parameters are found for initial snake at the beginning of the process. α and β parameters are defined between 0 and 1 (Neuenschwander et al. (1997)). The range between 0 and 1 is divided into 20 equal intervals. Total energy formula (equation 6) is executed for all combinations of twenty different values of alpha and beta. Then, the combination of α and β

values that give minimum energy is selected. Figure 34 shows calculation of alpha and beta parameters flow diagram. Consequently, α and β parameters that are found by using this method provided better and have more accurate results for road extraction as shown in Ribbon snake and Ziplock snake experiments as shown in figure 35(b). On the other hand, random and constant alpha and beta values cause false result as shown in figure 35(a).

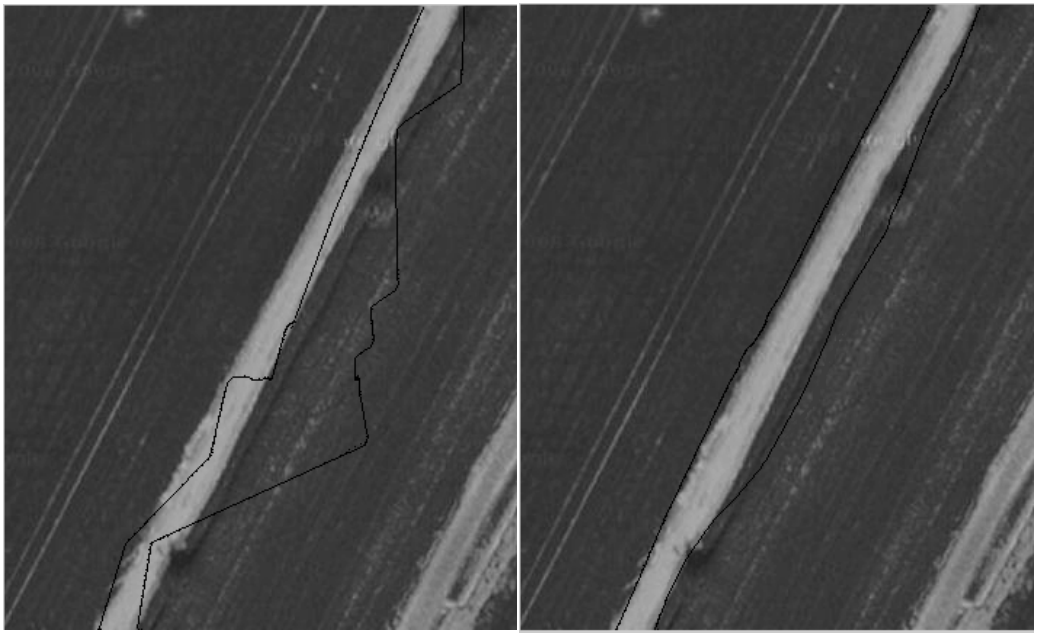

(a) (b)

Figure 35: (a) False detection with constant α and β (0.3 and 0.1) (b) True Detection with computed α and β (0.8773 and 0.7263 for first iteration)

4.6 Extraction of Crossing

Extraction of salient and non-salient roads provides not only minimum search space for crossings but also give some initial points to detect crossings. First of all, incomplete roads are searched, because these roads must have crossing. After that, center point of the end of the road that is incomplete is found as shown in figure 36.

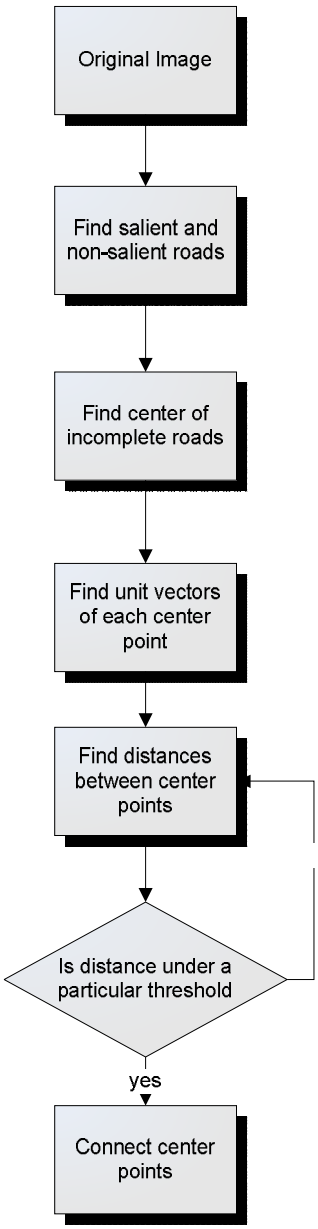

Figure 36: Extraction of Crossing Flow Diagram

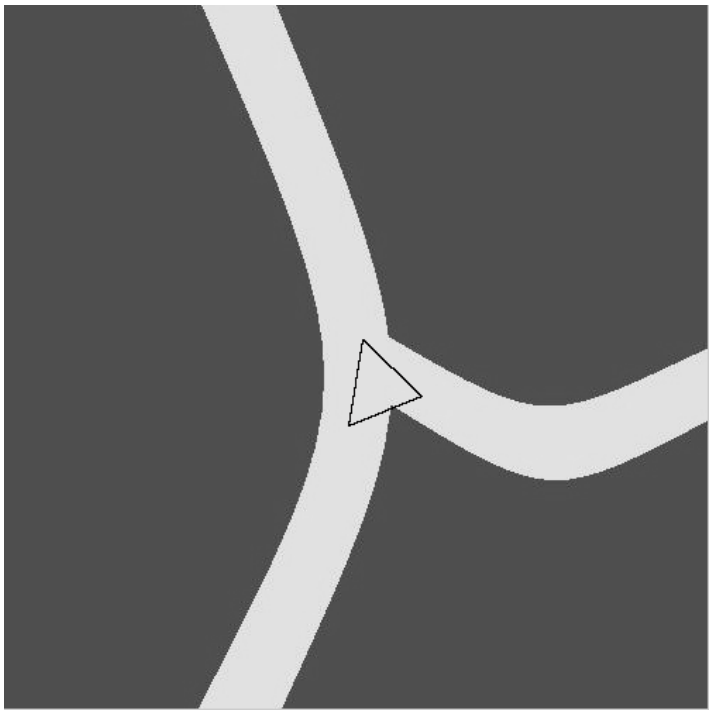

Figure 37: Extraction of Crossing in Synthetic Image

After end points of all incomplete roads are detected, the distances between them are calculated. If their distance is under a particular threshold, they are connected to each other as shown in figure 37 and 38. The threshold value is calculated as equal to the doubled road width. On the other hand, unit normal vectors of the center points are give a clue about road direction. Unit normal vector has been defined in chapter 3. Hence, center points of the lines are meet a center point that is the center of the crossing.

(a)

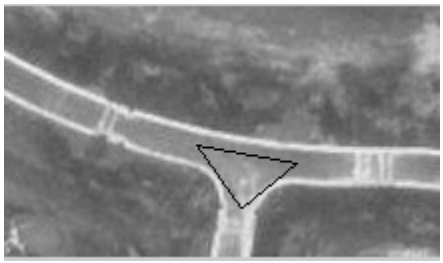

(b)

(c)

Figure 38: (a), (b) and (c) Extraction of crossings in real images

CHAPTER 5

CONCLUSIONS

In this thesis, Ziplock Snake and Ribbon Snake methods are tested and compared, some constant variables that are defined manually by user are supplied automatically with the new method that is defined and crossing extraction is supported by a new approach.

As defined in chapter 2, different algorithms from literature use different aerial and satellite images as depending on information requirements of algorithms while extraction of a road. In this study, all experimented gray level images are captured from Google Maps. They have 1-meter resolution. Especially high resolution images are preferred because their geometric properties and characteristics are obtained easily.

There are some constraints that are defined manually in past experiments of snake method. This study tries to convert these constraints to automatic. The elasticity and rigidity parameters are important geometric constraints for snake methods. In an automatic approach, elasticity and rigidity parameters change depending on the image or different contours of the same image. In the past applications such as in Laptev et al. (2000), these parameters have been defined constant at the beginning of the process. When the initial estimate of the ribbon is close to the final solution, this can be enforced by substituting these constant parameters with a factor λ. On the other hand, in this study, these parameters are calculated automatically from start to end of the application using their definitions as mentioned in Chapter 4.

Besides these, Gaussian kernel is applied for smoothing at the start of the Ziplock and Ribbon Snake method. As mentioned in Chapter 4, different sizes of Gaussian kernel cause different results. Thus, Gaussian Kernel size is experimented and obtained by using different resolution of images. And also different sizes of Gaussian kernel are tried for the same image to find out the kernel size giving the most satisfactory results.

Ribbon Snake is defined for only salient-road extraction in Laptev et al. (2000). But in this study, efficiency of Ribbon Snake is discussed for both salient-roads and non-salient roads. Ribbon Snake bases on energy minimization to extract a road (Kass et al. 1987). According to our experiments, we have some general results for ribbon snake. After true detection of initial snake location, Ribbon Snake is successful for salient and non-salient roads detection, too. But correctness and completeness has a little decreased in non-salient images. Ribbon Snake is not sufficient for only totally covered roads by other images. Elasticity and rigidity parameters have to find as true at all phases of the snake method.

Ziplock Snake is defined for non-salient road extraction (Laptev et al. 2000). In this study, efficiency of Ziplock method has been tested not only for non-salient roads but also for salient-roads. According to the experiments, Ziplock Snake does not give satisfactory results for complex images. For simple images that have straight road lines, Ziplock snake is succesful to detect roads. Ziplock Snake needs additional and correct control points to detect features (Neuenschwander et al. 1997). Also size of Gaussian kernel filter and the elasticity and rigidity parameters are affect the results of ziplock snake algorithms.

According to the experimental results, Ribbon Snake is more favorable than Ziplock Snake to extract salient and non-salient roads. While Ribbon snake and Ziplock snake gives similar results for extraction of salient roads, same thing can not be said for extraction of non-salient roads. Ziplock snake have much lower percentage of

correctness and lower percentage of completeness than Ribbon snake at extraction non-salient roads. Because of this, as mentioned above, Ziplock snake must be initialized by using more than two end points. Beside this, Ziplock snake might need new control points during optimization. On the contrast, Ribbon snake does not need any user intervention. Ziplock snake initialization step requires end points that are defined by output of the Ribbon snake method or users.

As mentioned above, Ribbon Snake is not sufficient for only totally covered roads by other images. Therefore, Ziplock and Ribbon Snake are used together for these images. Ribbon Snake detects uncovered parts of the image and then Ziplock Snake is initialized and optimized using ribbon snake end points for only detectable edge.

In crossing extraction, results of Ribbon method provide inputs and extractions of salient and non-salient roads provide not only minimum search space. As result of the Ribbon Snake application, there can be incomplete roads. The end points of the ribbon snake are obtained and distance between them is checked. If the number of the points that have distance less than the threshold is minimum three, these points are accepted as crossing points and connected to each other.

Last but not least, considering limitations and results of this study, some issues can be defined for future work. Firstly, Snake based approaches start with edge detection method. In this study, canny filter is applied but it is not effective for the complex images. Detect lines algorithm that is suggested and described by (Steger, 1998) can be developed. This algorithm provides to detect all relevant lines for the road detection. Thus, Snake methods can be applied to more complex images.

Number of iterations changes depending on the complexity and size of the images. Besides this, each iteration takes longer with more complex images. For large and complex images, the iteration times increase up to 3-5 hours. Thus, maximum image size is chosen 503x504 pixels as maximum because of the iteration time and speed of

extraction algorithm. The algorithm can be used for big images by optimizing algorithm and increasing its speed.

REFERENCES

Amini, J., Lucas, C., Sradjian, M. R., Azizi, A., & Sadeghian, S. (2002, April). Fuzzy Logic System for Road Identification Using Ikonos Images. *The Photogrammetric Record , 17(99)*, 493 - 503.

Bacher, U., & Mayer, H. (2005). Automatic Road Extraction from Multispectral High Resolution Satellite Images. *Object Extraction for 3D City Models, Road Databases and Traffic Monitoring - Concepts, Algorithms and Evaluation , 36(3/24)*, (pp. 29-34). Vienna, Austria: the ISPRS Workshop CMRT 2005.

Barsi, A., Heipke, C., & Willrich, F. (2002). Junction Extraction by Artificial Neural Network System-Jeans. *International Archives of Photogrammetry, Remote Sensing and Spatial Information Science (34) 3B* , 18-21.

Cohen, L. D. (1991). On Active Contour Models and Ballons. *In Computer Vision, Graphics, and Image Processing: Image Understanding* , 211-218.

Fua, P. (1997). Model-Based Optimization: An Approach to Fast, Accurate, and Consistent Site Modelling from Imagery. *RADIUS: Image Understanding for Intelligence Imagery* , 129-152.

Gardner, M. E., Roberts, D. A., Funk, C., & Noronha, V. (2001). Road Extraction from Aviris Using Spectral Mixture and Q-Tree Filter Techniques. *The Tenth JPL Airborne Earth Science Workshop*, (pp. 145-150). Pasadena, California.

Geraud, T., & Mouret, J. B. (2004, August 27). Fast Road Network Extraction in Satellite Images Using Mathematical Morphology and Markov Random Fields. *EURASIP Journal on Applied Signal Processing* , 2503-2514.

Henricsson, O., & Neuenschwander, W. (1994). Controlling Growing Snakes by Using Key-Points. *Pattern Recognition, Conference A: Vol. 1(9-13), Computer Vision & Image Processing.*, (pp. 68-73). Jerusalem, Israel: The 12th IAPR International Conference.

Hinz, M., Toennies, K. D., Grohmann, M., & Pohle, R. (2001). Active Double-Contour for Segmentation of Vessels in Digital Subtraction Angiography. *SPIE. Medical Imaging*, 1554-1562. San Diego, CA, USA.

Hsu, P.-H. (2007). Feature Extraction of Hyperspectral Images Using Wavelet and Matching Pursuit. *ISPRS Journal of Prohogrammetry & Remote Sensing, 62* , 78-92.

Hu, J., Razdan, A., Femiani, J., Wonka, P., & Cui, M. (2007). Fourier Shape Descriptors of Pixel Footprints for Road Extraction from Satellite Images. *2007 IEEE International Conference on Image Processing (ICIP 2007): Vol 1*, (pp. 49-52). San Antonio, Texas.

Kass, M., Witkin, A., & Terzopoulos, D. (1987). Snakes: Active Contour Models. *International Journal of Computer Vision, 1(4)* , 321-331.

Kim, T., Park, S. R., Kim, M. G., Jeong, S., & Kim, K. O. (2002). Semi Automatic Tracking of Road Centerlines from High Resolution Remote Sensing Data. *23rd Asian Conference on Remote Sensing (ACRS).* Kathmandu, Nepal.

Klang, D. (1998). Automatic Detection of Changes in Road Databases Using Satellite Imagery. *International Archives of Photogrammetry and Remote Sensing (ISPRS) Commission IV Symposium on GIS - Between Visions and Applications, Vol. 32/4*, (pp. 293-298). Stuttgart, Germany.

Laptev, I., Mayer, H., Lindeberg, T., Eckstein, W., Steger, C., & Baumgartner, A. (2000). Automatic extraction of roads from aerial images based on scale space and snakes. *Machine Vision and Applications , 12*, 23-31.

Lee, H.-Y., Park, W., & Lee, H.-K. (2000). Automatic Road Extraction from 1M-Resolution Satellite Images. *Proc. of International Symposium on Remote Sensing (ISRS2000)*, (pp. 177-183). Kyungju, Korea.

Leymarie, F., & Levine, M. D. (1993, June). Tracking Deformable Objects in the Plane Using an Active Contour Model. *IEEE Transactions on Pattern Analysis and Machine Intelligence* , *15(6)*, 617-634.

Li, X., Qiao, Y., Yi, W., & Guo, Z. (2003). The research of road extraction for high resolution satellite image. *Geoscience and Remote Sensing Symposium IGARSS,Vol. 6,* (pp. 3949-3951):*2003 IEEE International.*

Liu, H., Li, J., & Chapman, M. A. (2003, June). Automated Road Extraction from Satellite Imagery Using Hybrid Genetic Algorithms and Cluster Analysis. *Journal od Enviromental Informatics 1, 1* , 40-47.

Mayer, H., Laptev, I., Baumgartner, A., & Steger, C. (1997). Automatic Road Extraction Based on Multi-Scale Modeling, Context, and Snakes. *International Archives of Photogrammetry and Remote Sensing* , 106-113.

Neuenschwander, W. (1995). Elastic Deformable Contour and Surface Models for 2-D and 3-D Image Segmentation.Ph.D. Thesis. *Swiss Federal Institute of Technolody Zurich, Swithzerland*.

Neuenschwander, W., Fua, P., Szekely, G., & Kubler, O. (1995). Deformable Velcro Surfaces. *The Fifth International Conference on Computer Vision*, (pp. 828-833). Cambridge, MA, USA.

Neuenschwander, W., Fua, P., Szekely, G., & Kuebler, O. (1995). From Ziplock Snakes to Velcro(TM) Surfaces. In A. Gruen, O. Kuebler &P. Agouris (Eds.), *Automatic Extraction of Man-Made Objects from Aerial and Space Images* (pp. 105-114),ETH Zurich: Birkhauser Verlag Basel.

Neuenschwander, W., Fua, P., Szekely, G., & Kubler, O. (1997, December). Ziplock Snakes. *International Journal of Computer Vision, 26(3)* , 191-201.

Oddo, L. A., Douccette, P., & Agouris, P. (2000). Automated Road Extraction via the Hybridization of Self-organization and Model Based Techniques. *The 29th Applied Imagery Pattern Recognition Workshop (AIPR'00)*, (pp. 32-38), Los Amitos, CA, USA.

Peteri, R., Celle, J., & Ranchin, T. (2003). Detection and Extraction of Road Networks from High Resolution Satellite Images. *The IEEE International Conference on Image Processing (ICIP'03), Vol 1,* (pp. 301-304). Barcelona, Spain: IEEE.

Ravanbakhsh, M., Heipke, C., & Pakzad, K. (2007). Knowledge-based road junction extraction from high-resolution aerial images. *Urban Remote Sensing Joint Event, 2007*, (pp. 1-8). Paris, France.

Satellite Images and Geospatial Data for GIS & Mapping Applications. (2001). Retrieved 2009, from http://www.satimagingcorp.com/

Shukla, V., Chandrakanth, R., & Ramachandran, R. (2002). Semi-Automatic Road Extraction Algorithm for High Resolution Images Using Path Following Approach. *Indian Conference on Computer Vision, Graphics and Image Processing*, (pp. 231-236). Ahmadabad.

Steger, C. (1998, February). An Unbiased Detector of Curvilinear Structures. *IEEE Transactions on Pattern Analysis and Machine Intelligence* , 20(2), 113-125.

Wang, L., Qin, Q., Du, S., Chen, D., & Tao, J. (2005). Road Extraction from Remote Sensing Image Based on Multi-Resoluiton Analysis. *31st. International Symposium on Remote Sensing of Environment - Global Monitoring for Sustainability and Security.* Saint Petersburg, Russian.

Xu, C., & Prince, J. L. (1998). Snakes, Shapes, and GRadient Vector Flow. *IEEE Transactions on Image Proccesing* , 359-369.

Yu, Y. C., Lee, K. W., & Lee, B. G. (2003). Automatic Road Extraction by Gradient Direction Profile Algorithm (GDPA) using High-Resolution Satellite Imagery: Experiment Study. *Korean Journal of Remote Sensing* , 19(5), 393-402.

Zhang, C., Murai, S., & Baltsavias, E. (1999). Roas Network Detection by Mathematical Morphology. *3D Geospatial Data Production: Meeting Application Requirements* (pp. 185-200). Paris, France: Proc. of ISPRS Workshop.

Zhang, Q., & Couloigner, I. (2004, June). Automatic Road Change Detection and GIS Updating from High Spatial Remotely-Sensed Imagery. *Geo-Spatial Information Science* , 89-95.

Zhao, H., Kumagai, J., Nakagawa, M., & Shibasaki, R. (2002). Semi-Automatic Road Extraction from High-Resolution Satellite Image. *ISPRS. Photogrammetric Computer Vision* , A-406.

Zhou, J., Bischof, W. F., & Caelli, T. (2006). Road Tracking in Aerial Images Based on Human-Computer Interaction and Bayesian Filtering. *ISPRS Journal of Photogrammetry and Remote Sensing* , 61(2), 108-124.

APPENDICES

APPENDIX A: Earth Observation Satellites

Hyper Spectral

Hyper spectral images provide spectral data and detailed information about target spatial by scanning many channels across relatively narrow bandwidth. Many objects and substances have unique spectral characteristics and also unique spectral signatures. It is possible to distinguish properties of substance between spectrally similar objects clearly by using sensors to detect multiple wavelengths.

Hyperspectral Digital Imagery Collection Experiment (HYDICE)

Hyper spectral Digital Imagery Collection Experiment (HYDICE) was built by Hughes Danbury Optical Systems, Danbury, Conn., and delivered for integration into the Environmental Institute of Michigan's (ERIM) CV-580 aircraft in December 1994.

HYDICE collects data of 210 bands over the range 0.4-2.5 μm with a field of view 320 pixels wide at an IFOV (pixel size) of 1 to 4 m depending on the aircraft altitude and ground speed. The specifications are the same with AVIRIS, but this sensor had better signal noise than AVIRIS (1997).

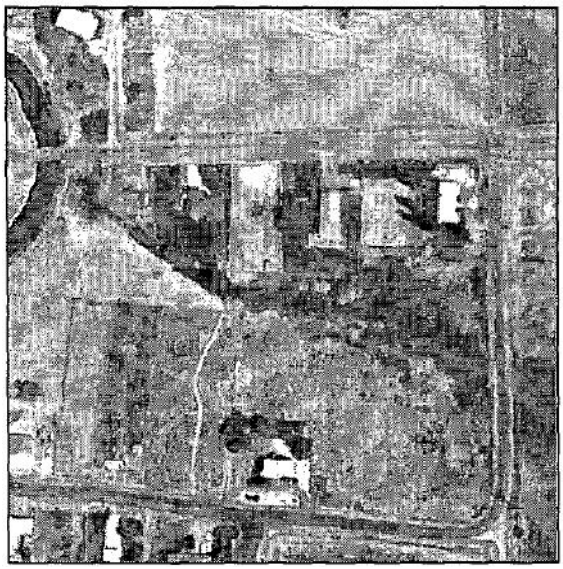

Figure App. A1: HYDICE Image. Courtesy of Oddo et al. (2000)

Airbone Visible/Infra-Red Imaging Spectrometer (AVIRIS)

AVIRIS is widely used imaging spectrometer. The first revision of it was finished in 1987. AVIRIS has 224 bands ranging from 0.380 to 2.45µm at a wavelength sensitive range of approximately 10nm.

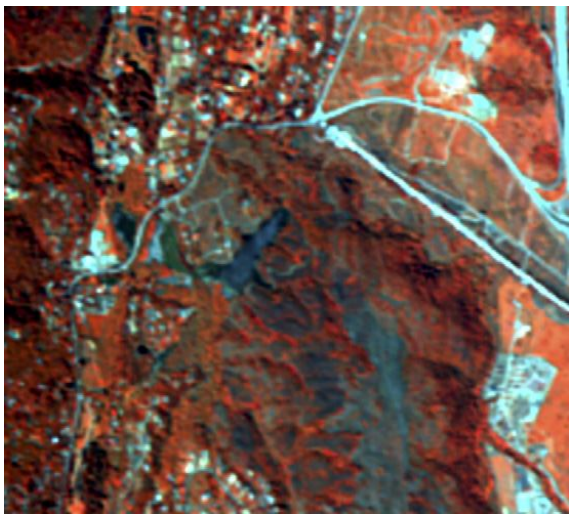

Figure App. A2: AVIRIS Image. Courtesy of Gardner et al. (2001)

IKONOS

IKONOS was originated under the Lockheed Martin Corporation as the Commercial Remote Sensing System (CRSS) satellite on April 1994. IKONOS can collect publicly available high resolution images at 1- and 4-meter resolution. It has two image sensors that take panchromatic (PAN) and multispectral (MS) imagery.

(a) (b)

Figure App. A3: (a) IKONOS Pan Image (b) IKONOS Image. Courtesy of Bacher & Mayer (2005) and Yu et al. (2003)

QUICKBIRD

QuickBird imagery is presented to the public by Digital Globe on October 2001. QuickBird satellites collect panchromatic imagery at 60-70 centimeter resolution and multispectral imagery at 2.4- and 2.8- meter resolution.

Figure App. A4: QUICKBIRD Image. Courtesy of Liu et al. (2003)

The QuickBird satellite collects both multi-spectral and panchromatic imagery concurrently, and 60cm Pan-sharpened composite products in natural or infrared colours are offered. Strips up to 250 km in length can be collected in a single pass. DigitalGlobe's QuickBird satellite provides the largest swath width, largest on-board storage, and highest resolution of any currently available commercial satellite. QuickBird is designed to efficiently and accurately image large areas with high geolocational accuracy. The QuickBird spacecraft is capable of acquiring over 75 million km^2 of imagery data annually (over three times the size of North America), allowing the archive to be populated and updated at unprecedented speed.

IRS (INDIAN REMOTE SENSING SATELLITE)

IRS is the first commercial earth observation satellite. It is developed by the Indian Space Research Organization in March 1988. It is separated as IRS-1A, 1B and 1C satellites. The IRS-1C satellite carries a PAN camera with 5.8m resolution and 70km swath. It is called as IRS-PAN.

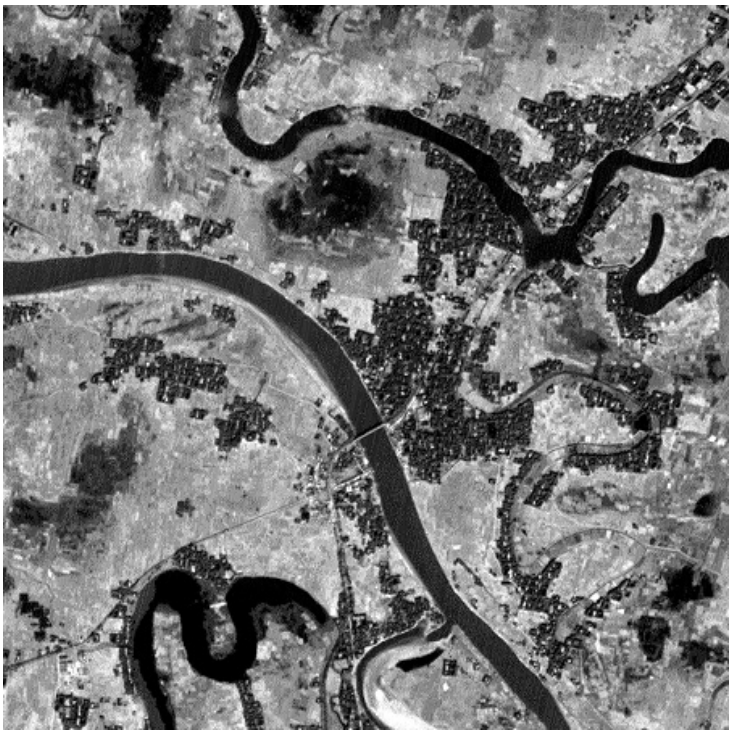

Figure App. A5: IRS-PAN Image. Courtesy of Satellite Images and Geospatial Data for GIS & Mapping Applications (2001)

SPOT-5

SPOT imagery covers a wide area (60 km x 60 km) and provides from 20-meter down to 2.5-meter resolution images for work on regional or local scales (from 1:100 000 to 1:10 000).

Figure App. A6: SPOT-5 Image. Courtesy of Satellite Images and Geospatial Data for GIS & Mapping Applications (2001)

APPENDIX B: Iterative Self Organizing Data Analysis Technique (ISODATA)

ISODATA is unsupervised classification algorithm. It is an iterative procedure that consists of three steps. Firstly initial cluster vector is chosen randomly. Secondly each pixel is classified as the closest cluster. In third step, a new cluster is obtained based on all pixels in a cluster. Second and third steps are iteratively repeated until distances of the clusters and percentage of the pixels in the clusters has no more change.

The ISODATA algorithm is similar to the k-means algorithm. ISODATA algorithm allows for different number of clusters while the number of clusters is taken as prior information in a k-means algorithm.

(a) **(b)**

Figure App. A7: (a) Test Image (b) Classified and Segmented Image by ISODATA. Courtesy of Zhang et al. (1999)